

OPTIMIZED SCHWARZ METHODS FOR HETEROGENEOUS HEAT TRANSFER PROBLEMS

MARTIN J. GANDER*, LIU-DI LU*, AND TINGTING WU†

Abstract. We present here nonoverlapping optimized Schwarz methods applied to heat transfer problems with heterogeneous diffusion coefficients. After a Laplace transform in time, we derive the error equation and obtain the convergence factor. The optimal transmission operators are nonlocal, and thus inconvenient to use in practice. We introduce three versions of local approximations for the transmission parameter, and provide a detailed analysis at the continuous level in each case to identify the best local transmission conditions. Numerical experiments are presented to illustrate the performance of each local transmission condition. As shown in our analysis, local transmission conditions, which are scaled appropriately with respect to the heterogeneous diffusion coefficients, are more efficient and robust especially when the discontinuity of the diffusion coefficient is large.

Key words. domain decomposition, optimized Schwarz methods, heterogenous heat equation, waveform relaxation, convergence analysis.

MSC codes. 65M55, 65M12, 65Y05,

1. Introduction. Hypersonic vehicles often travel at speeds exceeding five times of the speed of sound, and due to this extreme speed, these vehicles are exposed to high aerodynamic and thermal loads [1]. To ensure the safety of the vehicle, thermal protection structures must be designed and applied on the outer surface of the vehicle such that the inner structural temperature can stay in a sustainable range [16]. Hence, it is vital to study the heat transfer problems in these critical areas to obtain the temperature of the vehicle. A typical illustration of thermal protection structures is shown in Figure 1. Depending on the thermal protection techniques, several layers of materials can be applied over the vehicle skin, see e.g. [21] for a review. Each layer of the thermal protection structures may consist of different materials, such as aluminum and ceramic [15], and the diffusion coefficients can be very different from one material to another.

Numerical methods such as the finite element method and the boundary element method are often used to study such heat transfer problems, yielding reliable results [22, 6]. However, simulating heat transfer across various materials for critical areas of the vehicle can be time consuming. In [12, 13], the Reduced Models method is used to solve a nonlinear heat conduction problem, which drastically reduces the computing time. Given the geometric structure presented in Figure 1, nonoverlapping domain decomposition methods are natural candidates to introduce parallelism and accelerate the numerical solution of heat transfer problems with heterogenous diffusion coefficients. In [4], the authors developed a domain decomposition, or artificial subsectioning technique, along with a boundary–element method, to solve such heat conduction problems, showing the potential of domain decomposition.

The idea of domain decomposition was initially introduced by Hermann Amandus Schwarz in [20] to prove rigorously the existence of solution for Laplace problems. His method has then been developed as a computational tool with the arrival of parallel computing, see e.g. [7] for a historical review. Unlike dealing with homogeneous heat transfer problems where a continuous diffusion function is considered over the entire

*Section de Mathématiques, Université de Genève, rue du Conseil-Général 5-7, CP 64, 1205, Geneva, Switzerland (liudi.lu@unige.ch, martin.gander@unige.ch).

†School of Intelligent Equipment Engineering, Wuxi Taihu University, 214064, Wuxi, China (wtting@nuaa.edu.cn).

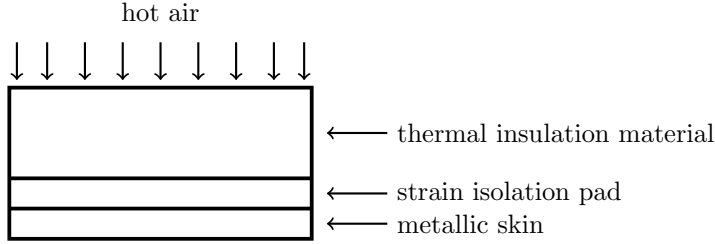


FIG. 1. *Illustration of thermal protection systems.*

44 domain, the heterogeneity of the material between two subdomains require special at-
 45 tention for heterogeneous heat transfer problems. In [19, 5], optimized Schwarz meth-
 46 ods are analyzed for solving heterogeneous Laplace problems. A reaction–diffusion
 47 problem with heterogeneous coefficients is studied in [10]. In [11], the authors con-
 48 sider using optimized Schwarz methods for solving unsymmetric advection–diffusion–
 49 reaction problems with strongly heterogeneous and anisotropic diffusion coefficients.
 50 The balancing Neumann–Neumann method is applied in [14] to treat linear elastic-
 51 ity systems with discontinuous coefficients. In [8], the authors extend the study to
 52 parabolic heat transfer problems with a constant diffusion coefficient using Dirichlet–
 53 Neumann and Neumann–Neumann waveform relaxation methods. Optimized Schwarz
 54 waveform relaxation methods are considered in [17, 18] to solve heterogeneous heat
 55 transfer problems. More recently, the authors in [3] analyzed at the continuous level
 56 of the Dirichlet–Neumann waveform relaxation method applied to heterogeneous heat
 57 transfer problems.

58 In the current study, we focus on the optimized Schwarz waveform relaxation
 59 methods to solve heat transfer problems with heterogeneous diffusion coefficients. It
 60 has already been observed in [17, 18] that the optimal transmission operators are
 61 nonlocal in time, and thus are inconvenient to use in practice. For this reason, we
 62 introduce here three local approximations of the transmission operators by taking
 63 into account the heterogeneous diffusion coefficients. As these local approximations
 64 are scaled differently with respect to the diffusion coefficients, we analyze in detail the
 65 min-max problem associated with each approximation and find analytical formulas
 66 for the optimized local transmission parameters. In particular, we show that the
 67 equioscillation property does not always lead to the best transmission parameters,
 68 as reported also in [8]. Thus, one needs to be careful when addressing the min-max
 69 problems to characterize the best transmission parameters. In addition, we also show
 70 the importance of using a good scaling to be able to derive an efficient and robust
 71 solver in the case of a largely heterogeneous media.

72 Our paper is organized as follows: in Section 2, we introduce the heterogeneous
 73 heat transfer problem and optimized Schwarz methods. A Laplace analysis is ap-
 74 plied to the error equations to determine the convergence factor. In Section 3, we
 75 introduce three local approximations of the optimal transmission operators and pro-
 76 vide a detailed analysis of each associated min-max problem. Numerical experiments
 77 are presented in Section 4 to illustrate the performance of these local transmission
 78 conditions.

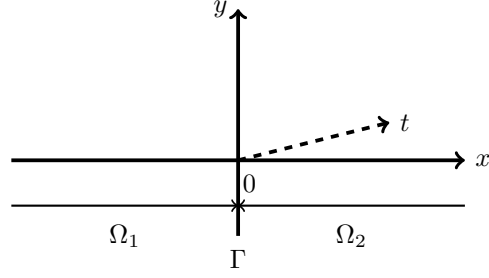


FIG. 2. 2D illustration of the decomposition.

79 **2. Model problem.** To model the heat transfer between different materials as
 80 shown in Figure 1, we consider the heterogeneous heat equation

$$\begin{aligned}
 (2.1) \quad & \partial_t u = \nabla \cdot (\nu \nabla u) + f && \text{in } Q := \Omega \times (0, T), \\
 & u = u_0 && \text{on } \Sigma_0 := \Omega \times \{0\}, \\
 & u = g && \text{on } \Sigma := \partial\Omega \times (0, T),
 \end{aligned}$$

82 where $\Omega \subset \mathbb{R}^d$, $d = 1, 2, 3$, with its boundary $\partial\Omega$, T is the fixed final time, ν is
 83 the heat diffusion function, f is the source term, u_0 is the initial condition, and g
 84 represents some Dirichlet boundary conditions. Furthermore, we consider a natural
 85 decomposition of two nonoverlapping subdomains Ω_1 and Ω_2 such that $\Omega_1 \cap \Omega_2 = \Gamma$,
 86 with Γ the interface between Ω_1 and Ω_2 , as shown in Figure 2. The heat diffusion
 87 function ν is assumed to be a piecewise constant function in space, where $\nu(\mathbf{x}) = \nu_j$
 88 for $\mathbf{x} \in \Omega_j$ with $\nu_j > 0$, $j = 1, 2$. For the sake of brevity, we will omit the initial and
 89 boundary conditions in the following.

90 The following physical coupling conditions are applied on the interface

$$91 \quad u_1 = u_2, \quad \nu_1 \partial_{\mathbf{n}_1} u_1 = -\nu_2 \partial_{\mathbf{n}_2} u_2, \quad \text{on } \Sigma_\Gamma := \Gamma \times (0, T),$$

92 to ensure the continuity of the solution and its normal flux between the subdomains.
 93 Here, the unit outward normal vector is denoted by \mathbf{n}_j . According to these two
 94 physical coupling conditions, we can write the optimized Schwarz method as: for the
 95 iteration index $k = 1, 2, \dots$, one solves

$$\begin{aligned}
 (2.2) \quad & \partial_t u_1^{k+1} = \nu_1 \Delta u_1^{k+1} + f_1 && \text{in } Q_1, \\
 & (\nu_1 \partial_{\mathbf{n}_1} + S_1) u_1^{k+1} = (\nu_2 \partial_{\mathbf{n}_1} + S_1) u_2^k && \text{on } \Sigma_\Gamma, \\
 & \partial_t u_2^{k+1} = \nu_2 \Delta u_2^{k+1} + f_2 && \text{in } Q_2, \\
 & (\nu_2 \partial_{\mathbf{n}_2} - S_2) u_2^{k+1} = (\nu_1 \partial_{\mathbf{n}_2} - S_2) u_1^{k+1} && \text{on } \Sigma_\Gamma,
 \end{aligned}$$

97 with $Q_j := \Omega_j \times (0, T)$, $j = 1, 2$. The system (2.2) is then completed by the given
 98 initial and boundary conditions of the problem (2.1). Here, f_j denotes the source term
 99 f restricted to the space-time domain Q_j , and S_j is a linear space-time operator. As
 100 illustrated in Figure 2, the decomposition is only in the x -direction, we thus consider
 101 in the following the one dimensional case, i.e., $\Omega = \mathbb{R}$, to focus on the transmission
 102 condition at the interface $x = 0$. This will simplify the computations and allow us to
 103 obtain a more compact analytical form. In this case, the two space-time subdomains
 104 are $Q_1 = (-\infty, 0) \times (0, T)$ and $Q_2 = (0, \infty) \times (0, T)$, and the linear operator S_j

105 is only related to the time variable. Although the following convergence analyses
 106 are for the two-subdomain case only, our numerical experiments in Section 4 for
 107 multiple subdomains with different choices of the diffusion coefficient ν show that our
 108 theoretical results are also very useful in more general situations.

109 **2.1. Laplace Analysis.** To understand the convergence behavior of the opti-
 110 mized Schwarz algorithm (2.2), we will study the associated error equations with
 111 solutions which go to zero when x goes to infinity. We denote the error by $e_j^k(\mathbf{x}, t) :=$
 112 $u(\mathbf{x}, t) - u_j^k(\mathbf{x}, t)$, $j = 1, 2$, which satisfies by linearity the equation

$$113 \quad \partial_t e_j^k = \partial_t(u - u_j^k) = \nu_j \Delta(u - u_j^k) = \nu_j \Delta e_j^k \quad \text{in } Q_j.$$

114 To focus on the transmission condition in space at the interface Γ , we apply a Laplace
 115 transform in the time variable t ,

$$116 \quad \hat{e}_j^k(\mathbf{x}, s) := \mathcal{L}\{e_j^k(\mathbf{x}, t)\} = \int_0^\infty e_j^k(\mathbf{x}, t) e^{-st} dt,$$

117 where $s \in \mathbb{C}$ is a complex number. We study the associated error equation of (2.2)
 118 after the Laplace transform, that is,

$$119 \quad (2.3) \quad \begin{aligned} s\hat{e}_1^{k+1}(x, s) &= \nu_1 \partial_{xx} \hat{e}_1^{k+1}(x, s) && \text{in } Q_1, \\ (\nu_1 \partial_x + \sigma_1(s))\hat{e}_1^{k+1}(0, s) &= (\nu_2 \partial_x + \sigma_1(s))\hat{e}_2^k(0, s), \\ s\hat{e}_2^{k+1}(x, s) &= \nu_2 \partial_{xx} \hat{e}_2^{k+1}(x, s) && \text{in } Q_2, \\ (\nu_2 \partial_x - \sigma_2(s))\hat{e}_2^{k+1}(0, s) &= (\nu_1 \partial_x - \sigma_2(s))\hat{e}_1^{k+1}(0, s), \end{aligned}$$

120 where $\sigma_j(s)$ are the Laplace symbols of the operators S_j . The general solutions are
 121 given by

$$122 \quad \hat{e}_1^{k+1}(x, s) = C_1^{k+1}(s) \exp\left(\frac{\sqrt{s}}{\sqrt{\nu_1}} x\right), \quad \hat{e}_2^{k+1}(x, s) = C_2^{k+1}(s) \exp\left(-\frac{\sqrt{s}}{\sqrt{\nu_2}} x\right).$$

123 Applying the transmission conditions in (2.3), we obtain the convergence factor for
 124 $\{\hat{e}_j^k\}_{k=1,2,\dots}$

$$125 \quad (2.4) \quad \rho(s, \sigma_1, \sigma_2) := \left| \frac{\sigma_1(s) - \sqrt{\nu_2} \sqrt{s}}{\sigma_1(s) + \sqrt{\nu_1} \sqrt{s}} \cdot \frac{\sigma_2(s) - \sqrt{\nu_1} \sqrt{s}}{\sigma_2(s) + \sqrt{\nu_2} \sqrt{s}} \right|.$$

126 It is straightforward from (2.4) that we can get optimal convergence by choosing

$$127 \quad (2.5) \quad \sigma_1(s) = \sqrt{\nu_2} \sqrt{s}, \quad \sigma_2(s) = \sqrt{\nu_1} \sqrt{s}.$$

128 This leads to convergence in two iterations, since the errors at iteration $k = 2$ vanish.
 129 However, the best choice is nonlocal in time due to the term \sqrt{s} , and it is expensive to
 130 compute and inconvenient for the implementation. Therefore, the goal of the current
 131 study is to find good local approximations of $\sigma_j(s)$ that can still give fast convergence.

132 **3. Approximation of the optimal operators.** The idea is to fix a class of
 133 possible transmission conditions \mathcal{C} and uniformly optimize the convergence factor
 134 over a range of frequencies for our problem. This corresponds to solve the min-max
 135 problem

$$136 \quad (3.1) \quad \min_{\sigma_j \in \mathcal{C}} \left(\max_s \rho(s, \sigma_1, \sigma_2) \right).$$

137 To find local approximations of $\sigma_j(s)$, we consider in the following $\sigma_j \in \mathbb{R}$, independent
 138 of the time variable. In this way, the convergence factor (2.4) becomes

$$139 \quad (3.2) \quad \rho(s, \sigma_1, \sigma_2) := \left| \frac{\sigma_1 - \sqrt{\nu_2} \sqrt{s}}{\sigma_1 + \sqrt{\nu_1} \sqrt{s}} \cdot \frac{\sigma_2 - \sqrt{\nu_1} \sqrt{s}}{\sigma_2 + \sqrt{\nu_2} \sqrt{s}} \right|.$$

140 For the Laplace transform, we have $s = \eta + i\omega$ with $\eta, \omega \in \mathbb{R}$. This implies that

$$141 \quad \sqrt{s} = \sqrt{\eta + i\omega} = \sqrt{\frac{\eta + \sqrt{\eta^2 + \omega^2}}{2}} \pm i \sqrt{\frac{-\eta + \sqrt{\eta^2 + \omega^2}}{2}}.$$

142 Since \sqrt{s} is an even function of the imaginary part ω , the convergence factor ρ is
 143 also an even function of ω . Therefore, we only consider $\omega \geq 0$ in the analysis. Now
 144 the imaginary part $\omega = 0$ corresponds to a constant function in time, and since the
 145 error function $e_j^k(x, t)$ equals zero at $t = 0$, the constant function cannot be part of
 146 the error function in the iteration. From a numerical viewpoint, when solving the
 147 problem in the time interval $[0, T]$, we can heuristically state that $\omega \in [\omega_{\min}, \omega_{\max}]$,
 148 where the smallest frequency ω_{\min} is $\frac{\pi}{2T}$, and the largest frequency is related to the
 149 time step Δt , that is $\omega_{\max} = \frac{\pi}{\Delta t}$. We refer to [9, Figure 3.17] for more details about
 150 this statement. Thus, we can set $\eta = 0$ as we only solve the min-max problem (3.1)
 151 away from $\omega = 0$. Denoting by $\tilde{\omega} := \sqrt{\frac{\omega}{2}}$, we get

$$152 \quad \sqrt{s} = \sqrt{\frac{\omega}{2}} \pm i \sqrt{\frac{\omega}{2}} = \tilde{\omega} \pm i\tilde{\omega}.$$

153 The new parameter $\tilde{\omega} \in [\tilde{\omega}_1, \tilde{\omega}_2]$ with $\tilde{\omega}_1 := \sqrt{\frac{\omega_{\min}}{2}} = \sqrt{\frac{\pi}{4T}}$ and $\tilde{\omega}_2 := \sqrt{\frac{\omega_{\max}}{2}} =$
 154 $\sqrt{\frac{\pi}{2\Delta t}}$. The convergence factor (3.2) can then be simplified to

$$155 \quad (3.3) \quad \rho(\tilde{\omega}, \sigma_1, \sigma_2) = \sqrt{\frac{(\sigma_1 - \sqrt{\nu_2} \tilde{\omega})^2 + \nu_2 \tilde{\omega}^2}{(\sigma_1 + \sqrt{\nu_1} \tilde{\omega})^2 + \nu_1 \tilde{\omega}^2} \cdot \frac{(\sigma_2 - \sqrt{\nu_1} \tilde{\omega})^2 + \nu_1 \tilde{\omega}^2}{(\sigma_2 + \sqrt{\nu_2} \tilde{\omega})^2 + \nu_2 \tilde{\omega}^2}}.$$

156 To find good local operators, we can restrict the range of σ_j . More precisely, suppose
 157 $\sigma_1 > 0$ and substitute σ_1 by $-\sigma_1$ in (3.3), we have

$$158 \quad \rho(\tilde{\omega}, -\sigma_1, \sigma_2) = \sqrt{\frac{(\sigma_1 + \sqrt{\nu_2} \tilde{\omega})^2 + \nu_2 \tilde{\omega}^2}{(\sigma_1 - \nu_1 \tilde{\omega}^2) + \nu_1 \tilde{\omega}^2} \cdot \frac{(\sigma_2 - \sqrt{\nu_1} \tilde{\omega})^2 + \nu_1 \tilde{\omega}^2}{(\sigma_2 + \sqrt{\nu_2} \tilde{\omega})^2 + \nu_2 \tilde{\omega}^2}}.$$

159 This implies that $\rho(\tilde{\omega}, -\sigma_1, \sigma_2) > \rho(\tilde{\omega}, \sigma_1, \sigma_2)$, when $\sigma_1 > 0$. Therefore, for fast
 160 convergence, $\sigma_1 > 0$ should be chosen. In a similar way, we can restrict the range of
 161 σ_2 to $\sigma_2 > 0$. The min-max problem (3.1) thus becomes

$$162 \quad (\text{P}) \quad \min_{\sigma_j > 0} \left(\max_{\tilde{\omega}_1 \leq \tilde{\omega} \leq \tilde{\omega}_2} \rho(\tilde{\omega}, \sigma_1, \sigma_2) \right).$$

163 Before analyzing the convergence of several choices for local transmission parameters
 164 σ_j , we give sufficient conditions on σ_j that will guarantee convergence of the optimized
 165 Schwarz algorithm (2.3).

166 **THEOREM 3.1** (Sufficient condition). *Under the conditions*

$$167 \quad \begin{aligned} 0 < \sigma_2 \leq \sigma_1, & \quad \text{if } \nu_1 < \nu_2, \\ 0 < \sigma_1 \leq \sigma_2, & \quad \text{if } \nu_2 < \nu_1, \end{aligned}$$

168 the optimized Schwarz algorithm (2.3) converges for all $\tilde{\omega} \in [\tilde{\omega}_1, \tilde{\omega}_2]$ and the conver-
 169 gence factor (3.3) satisfies

$$170 \quad \rho(\tilde{\omega}, \sigma_1, \sigma_2) < 1.$$

171 *Proof.* To guarantee convergence of the optimized Schwarz algorithm (2.3), we
 172 want from (3.3) that

$$173 \quad \rho(\tilde{\omega}, \sigma_1, \sigma_2) = \sqrt{\frac{(\sigma_1 - \sqrt{\nu_2 \tilde{\omega}})^2 + \nu_2 \tilde{\omega}^2}{(\sigma_1 + \sqrt{\nu_1 \tilde{\omega}})^2 + \nu_1 \tilde{\omega}^2} \cdot \frac{(\sigma_2 - \sqrt{\nu_1 \tilde{\omega}})^2 + \nu_1 \tilde{\omega}^2}{(\sigma_2 + \sqrt{\nu_2 \tilde{\omega}})^2 + \nu_2 \tilde{\omega}^2}} < 1,$$

174 which can be simplified to

$$175 \quad \tilde{\omega}(\sqrt{\nu_1} - \sqrt{\nu_2})(\sigma_1 - \sigma_2) - \sigma_1 \sigma_2 - 2\sqrt{\nu_1 \nu_2} \tilde{\omega}^2 < 0.$$

176 A simple sufficient condition for this inequality to hold is $(\sqrt{\nu_1} - \sqrt{\nu_2})(\sigma_1 - \sigma_2) \leq 0$,
 177 which is clearly not a necessary condition. This concludes the proof. \square

178 In the following subsections, we consider three choices for the transmission pa-
 179 rameters σ_j and their related min-max problems (P). In all cases, Theorem 3.1 will be
 180 satisfied to guarantee convergence of optimized Schwarz algorithm (2.3) when using
 181 these local transmission conditions. To treat the min-max problems (P) and find the
 182 best transmission parameters σ_j , we follow three steps similar as used in [5]:

- 183 1. restrict the range of the transmission parameter σ_j with respect to the fre-
 184 quencies $\tilde{\omega}_1$ and $\tilde{\omega}_2$;
- 185 2. identify possible local maximum points $\tilde{\omega}$ for the min-max problem (P);
- 186 3. analyze how these local maxima behave when the transmission parameters
 187 σ_j vary to find the minimizers.

188 **3.1. Local transmission parameter: Version I.** We first consider the trans-
 189 mission parameters σ_j with one free variable p ,

$$190 \quad (3.4) \quad \sigma_1 = \sigma_2 = \sqrt{\nu_2} p, \quad p > 0,$$

191 where we scale both parameters with only one diffusion coefficient ν_2 . Note that
 192 one could also scale with respect to ν_1 instead. Here, the parameter p is chosen to be
 193 positive such that the hypothesis in Theorem 3.1 is satisfied, and thus the convergence
 194 of (2.3) is guaranteed. Although this choice may not be the best one, as the optimal
 195 transmission operators (2.5) are scaled with respect to both diffusion coefficients ν_1
 196 and ν_2 , we still analyze this very simple choice both for completeness and comparison
 197 purposes. The convergence factor (3.3) for this choice is given by

$$198 \quad (3.5) \quad \rho(\tilde{\omega}, p) = \sqrt{\frac{(p - \tilde{\omega})^2 + \tilde{\omega}^2}{(p + \mu \tilde{\omega})^2 + \mu^2 \tilde{\omega}^2} \cdot \frac{(p - \mu \tilde{\omega})^2 + \mu^2 \tilde{\omega}^2}{(p + \tilde{\omega})^2 + \tilde{\omega}^2}},$$

199 where $\mu := \sqrt{\frac{\nu_1}{\nu_2}}$ such that μ^2 is the ratio of the two diffusion coefficients. In the
 200 following, we only consider the case when $\mu > 1$, since the case when $\mu < 1$ can be
 201 converted to the case $\mu > 1$ by interchanging ν_1 and ν_2 . We now want to find the best
 202 value of the transmission parameter p such that the convergence factor (3.5) can be
 203 minimized uniformly over the range of frequencies $[\tilde{\omega}_1, \tilde{\omega}_2]$. In this way, the min-max
 204 problem (P) becomes

$$205 \quad (P1) \quad \min_{p>0} \left(\max_{\tilde{\omega}_1 \leq \tilde{\omega} \leq \tilde{\omega}_2} \rho(\tilde{\omega}, p) \right).$$

206 We first show how to restrict the range for the transmission parameter p .

207 LEMMA 3.2 (Restrict parameter p). *The min-max problem (P1) is equivalent to*
 208 *the problem where we minimize the convergence factor when the transmission param-*
 209 *eter p is in the interval*

$$210 \quad p \in \begin{cases} [\sqrt{2\mu\tilde{\omega}_1}, \sqrt{2\mu\tilde{\omega}_2}], & \text{if } \mu \leq 2 + \sqrt{3}, \\ [\tilde{\omega}_1\sqrt{(\mu-1)^2 - \delta}, \tilde{\omega}_2\sqrt{(\mu-1)^2 + \delta}], & \text{if } \mu > 2 + \sqrt{3}, \end{cases}$$

211 with $\delta = \sqrt{(\mu^2 - 4\mu + 1)(\mu^2 + 1)}$.

212 *Proof.* We first take the partial derivative of the convergence factor (3.5) with
 213 respect to the transmission parameter p ,

$$214 \quad (3.6) \quad \text{sign}\left(\frac{\partial\rho}{\partial p}\right) = \text{sign}\left((p^2 - 2\mu\tilde{\omega}^2)(p^4 - 2p^2(\mu-1)^2\tilde{\omega}^2 + 4\mu^2\tilde{\omega}^4)\right).$$

215 The discriminant of the second polynomial $p^4 - 2p^2(\mu-1)^2\tilde{\omega}^2 + 4\mu^2\tilde{\omega}^4$ is

$$216 \quad (3.7) \quad \Delta = 4\tilde{\omega}^4(\mu^2 - 4\mu + 1)(\mu^2 + 1).$$

217 According to the value of the discriminant (3.7), we divide the analysis into two cases.

218 **Case 1** $\Delta \leq 0$: In this case, we find from (3.7) that $\mu \leq 2 + \sqrt{3}$, and the
 219 polynomial $p^4 - 2p^2(\mu-1)^2\tilde{\omega}^2 + 4\mu^2\tilde{\omega}^4$ is always nonnegative. Thus, we have

$$220 \quad \text{sign}\left(\frac{\partial\rho}{\partial p}\right) = \text{sign}(p^2 - 2\mu\tilde{\omega}^2) = \begin{cases} \text{positive,} & \text{if } p > \sqrt{2\mu\tilde{\omega}}, \\ \text{negative,} & \text{if } p < \sqrt{2\mu\tilde{\omega}}. \end{cases}$$

221 We observe that increasing p will make the convergence factor (3.5) decrease when
 222 $p < \sqrt{2\mu\tilde{\omega}_1}$, and decreasing p will make the convergence factor (3.5) decrease when
 223 $p > \sqrt{2\mu\tilde{\omega}_2}$. Therefore, p should be in the range of $[\sqrt{2\mu\tilde{\omega}_1}, \sqrt{2\mu\tilde{\omega}_2}]$ to minimize the
 224 convergence factor ρ .

225 **Case 2** $\Delta > 0$: In this case, we find from (3.7) that $\mu > 2 + \sqrt{3}$. From (3.6), we
 226 then find

$$227 \quad \text{sign}\left(\frac{\partial\rho}{\partial p}\right) = \begin{cases} \text{negative,} & \text{if } 0 < p^2 < \tilde{\omega}^2((\mu-1)^2 - \delta), \\ \text{positive,} & \text{if } \tilde{\omega}^2((\mu-1)^2 - \delta) < p^2 < 2\mu\tilde{\omega}^2, \\ \text{negative,} & \text{if } 2\mu\tilde{\omega}^2 < p^2 < \tilde{\omega}^2((\mu-1)^2 + \delta), \\ \text{positive,} & \text{if } p^2 > \tilde{\omega}^2((\mu-1)^2 + \delta). \end{cases}$$

228 Similar to **Case 1**, p^2 should be in the range of $[\tilde{\omega}_1^2((\mu-1)^2 - \delta), \tilde{\omega}_2^2((\mu-1)^2 + \delta)]$
 229 to minimize the convergence factor ρ . This completes the proof. \square

230 We now study the behavior of the convergence factor (3.5) as a function of $\tilde{\omega}$.

231 LEMMA 3.3 (Local maxima of $\tilde{\omega}$). *Denoting by $\tilde{\omega}_c := \frac{p}{\sqrt{2\mu}}$, we can write the*
 232 *maximum of the convergence factor (3.5) as*

$$233 \quad \begin{aligned} & \text{if } \mu \leq 2 + \sqrt{3}, \quad \max_{\tilde{\omega}_1 \leq \tilde{\omega} \leq \tilde{\omega}_2} \rho(\tilde{\omega}, p) = \max\{\rho(\tilde{\omega}_1, p), \rho(\tilde{\omega}_2, p)\}, \\ & \text{if } \mu > 2 + \sqrt{3}, \quad \max_{\tilde{\omega}_1 \leq \tilde{\omega} \leq \tilde{\omega}_2} \rho(\tilde{\omega}, p) = \begin{cases} \max\{\rho(\tilde{\omega}_1, p), \rho(\tilde{\omega}_2, p)\}, & \tilde{\omega}_c \notin [\tilde{\omega}_1, \tilde{\omega}_2], \\ \max\{\rho(\tilde{\omega}_1, p), \rho(\tilde{\omega}_c, p), \rho(\tilde{\omega}_2, p)\}, & \tilde{\omega}_c \in [\tilde{\omega}_1, \tilde{\omega}_2]. \end{cases} \end{aligned}$$

234 *Proof.* Taking the partial derivative of the convergence factor (3.5) with respect
235 to the frequency $\tilde{\omega}$, we find

$$236 \quad \text{sign}\left(\frac{\partial \rho}{\partial \tilde{\omega}}\right) = \text{sign}\left(- (p^2 - 2\mu\tilde{\omega}^2)(p^4 - 2p^2(\mu - 1)^2\tilde{\omega}^2 + 4\mu^2\tilde{\omega}^4)\right),$$

237 which has the opposite sign of (3.6). Given this similarity between the two partial
238 derivatives, we also consider two cases.

239 **Case 1** $\mu \leq 2 + \sqrt{3}$: In this case, the discriminant (3.7) is non-positive, and the
240 polynomial $p^4 - 2p^2(\mu - 1)^2\tilde{\omega}^2 + 4\mu^2\tilde{\omega}^4$ is always nonnegative. Then, we have

$$241 \quad \text{sign}\left(\frac{\partial \rho}{\partial \tilde{\omega}}\right) = \text{sign}(2\mu\omega^2 - p^2) = \begin{cases} \text{negative,} & \text{if } \tilde{\omega}_1 < \tilde{\omega} < \tilde{\omega}_c, \\ \text{positive,} & \text{if } \tilde{\omega}_c < \tilde{\omega} < \tilde{\omega}_2, \end{cases}$$

242 meaning that the maximum of the convergence factor $\rho(\tilde{\omega}, p)$ in the range $[\tilde{\omega}_1, \tilde{\omega}_2]$ is
243 $\max\{\rho(\tilde{\omega}_1, p), \rho(\tilde{\omega}_2, p)\}$.

244 **Case 2** $\mu > 2 + \sqrt{3}$: In this case, we observe that,

$$245 \quad \text{sign}\left(\frac{\partial \rho}{\partial \tilde{\omega}}\right) = \begin{cases} \text{negative,} & \text{if } 0 < \tilde{\omega}^2 < \frac{\tilde{\omega}_c^2}{2\mu}((\mu - 1)^2 - \delta), \\ \text{positive,} & \text{if } \frac{\tilde{\omega}_c^2}{2\mu}((\mu - 1)^2 - \delta) < \tilde{\omega}^2 < \tilde{\omega}_c^2, \\ \text{negative,} & \text{if } \tilde{\omega}_c^2 < \tilde{\omega}^2 < \frac{\tilde{\omega}_c^2}{2\mu}((\mu - 1)^2 + \delta), \\ \text{positive,} & \text{if } \tilde{\omega}^2 > \frac{\tilde{\omega}_c^2}{2\mu}((\mu - 1)^2 + \delta). \end{cases}$$

246 As the value of $\tilde{\omega}_c = \frac{p}{\sqrt{2\mu}}$ might fall outside the interval $[\tilde{\omega}_1, \tilde{\omega}_2]$, the maximum of
247 the convergence factor $\rho(\tilde{\omega}, p)$ will then be taken according to the value of $\tilde{\omega}_c$. This
248 concludes the proof. \square

249 With the help of Lemma 3.2 and Lemma 3.3, we can now identify the possible
250 choices of the optimized parameter p according to the ratio μ .

251 **THEOREM 3.4** (Optimized transmission parameter: $\mu \leq 2 + \sqrt{3}$). *The value p*
252 *minimizing the convergence factor (3.5) is $p^* = \sqrt{2\mu\tilde{\omega}_1\tilde{\omega}_2}$.*

253 *Proof.* In this case, the maximum in the min-max problem (P1) is determined by
254 Lemma 3.3 as $\max\{\rho(\tilde{\omega}_1, p), \rho(\tilde{\omega}_2, p)\}$, and we need to find its minimum with respect
255 to p . According to (3.6), it is easy to check that for the transmission parameter
256 $p \in [\sqrt{2\mu\tilde{\omega}_1}, \sqrt{2\mu\tilde{\omega}_2}]$, the convergence factor $\rho(\tilde{\omega}_1, p)$ is increasing with respect to p ,
257 and $\rho(\tilde{\omega}_2, p)$ is decreasing with respect to p . Using then the equioscillation principle,
258 the convergence factor can be minimized when its value at ω_1 and ω_2 are equal, i.e.,
259 $\rho(\tilde{\omega}_1, p^*) = \rho(\tilde{\omega}_2, p^*)$, which leads to the unique optimized parameter $p^* = \sqrt{2\mu\tilde{\omega}_1\tilde{\omega}_2}$. \square

260 **THEOREM 3.5** (Optimized transmission parameter: $\mu > 2 + \sqrt{3}$). *Let us denote*
261 *by*

$$262 \quad R_c := \rho(\tilde{\omega}_c, p) = \rho\left(\frac{p}{\sqrt{2\mu}}, p\right) = \sqrt{\frac{(\sqrt{2\mu} - 1)^2 + 1}{(\sqrt{2} + \sqrt{\mu})^2 + \mu} \frac{(\sqrt{2} - \sqrt{\mu})^2 + \mu}{(\sqrt{2\mu} + 1)^2 + 1}}, \quad k_r := \frac{\tilde{\omega}_2}{\tilde{\omega}_1},$$

263 and introduce two functions of μ ,

$$264 \quad h_1(\mu) := \frac{\mu^2 + 1 + \sqrt{(\mu^2 - 4\mu + 1)(\mu^2 + 4\mu + 1)}}{4\mu}, \quad h_2(\mu) := \frac{(\mu - 1)^2 + \delta}{2\mu}.$$

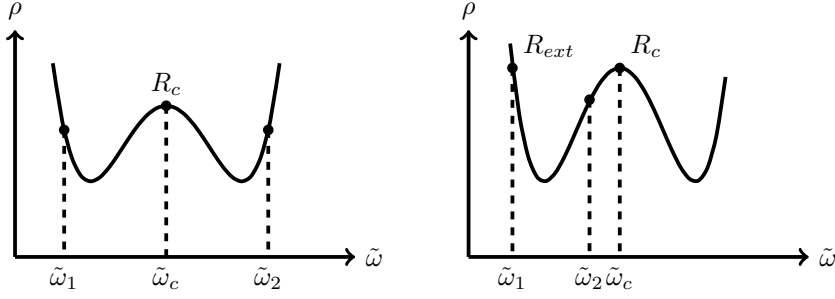


FIG. 3. Illustration of the convergence factor ρ as a function of $\tilde{\omega}$ with different values of the parameter p . Left: $p \in I_c$. Right: $p \in I_r$.

Moreover, we divide the possible range of p into three intervals,

$$I_l := [\tilde{\omega}_1 \sqrt{(\mu - 1)^2 - \delta}, \sqrt{2\mu\tilde{\omega}_1}], \quad I_c := [\sqrt{2\mu\tilde{\omega}_1}, \sqrt{2\mu\tilde{\omega}_2}],$$

$$I_r := [\sqrt{2\mu\tilde{\omega}_2}, \tilde{\omega}_2 \sqrt{(\mu - 1)^2 + \delta}].$$

According to the value of the ratio k_r , we have the following three cases:

- (i) if $k_r > h_2(\mu)$, then one value of the parameter p minimizing the convergence factor is $p^* = \sqrt{2\mu\tilde{\omega}_1\tilde{\omega}_2} \in I_c$. This optimized parameter p^* is unique when $\rho(\tilde{\omega}_1, p^*) \geq R_c$. Otherwise, the minimum of the convergence factor is also attained for any p chosen in a closed interval around p^* ;
- (ii) if $h_1(\mu) < k_r \leq h_2(\mu)$, the minimum of the convergence factor is attained for any p chosen in a closed interval around p^* ;
- (iii) if $k_r \leq h_1(\mu)$, then the minimum is attained with two distinct values p_l and p_r , which can be obtained by solving $\rho(\tilde{\omega}_1, p) = \rho(\tilde{\omega}_2, p)$ in two intervals I_l and I_r respectively. Furthermore, these two distinct minimizers are the two positive roots of the fourth-order polynomial

$$(3.8) \quad \frac{p^4}{2} + (\mu\tilde{\omega}_2 - \tilde{\omega}_1)(\tilde{\omega}_2 - \mu\tilde{\omega}_1)p^2 + 2\mu^2\tilde{\omega}_1^2\tilde{\omega}_2^2 = 0.$$

Proof. The main idea is to look at three intervals I_l , I_c and I_r and find the best value of the transmission parameter p in each interval separately. Let us start with the case when $p \in I_c$, where we have the interior local maximizer $\tilde{\omega}_c = \frac{p}{\sqrt{2\mu}}$ lying in the interval $[\tilde{\omega}_1, \tilde{\omega}_2]$, as shown in Figure 3 on the left. Then using Lemma 3.3, the maximum in the min-max problem (P1) is given by

$$\max_{\tilde{\omega}_1 \leq \tilde{\omega} \leq \tilde{\omega}_2} \rho(\tilde{\omega}, p) = \max \{ \rho(\tilde{\omega}_1, p), R_c, \rho(\tilde{\omega}_2, p) \}.$$

In this case, we can show that one of the minimal convergence factors can be obtained through the equioscillation property, i.e., $\rho(\tilde{\omega}_1, p) = \rho(\tilde{\omega}_2, p)$, which leads to one of the optimized parameters p^* . We also observe that the interior local maximum R_c might be greater than the convergence value at the endpoints with $p = p^*$, i.e., $R_c > \rho(\tilde{\omega}_1, p^*) = \rho(\tilde{\omega}_2, p^*)$. In that case, the maximum in the min-max problem (P1) is always R_c , and from its definition, R_c is constant with respect to p . Thus, the minimum of the convergence factor is also attained when we move the parameter p in an interval around p^* .

293 Solving the equality $\rho(\tilde{\omega}_1, p) = \rho(\tilde{\omega}_2, p)$, we obtain a product of two polynomials
 294 of p ,

$$295 \quad (3.9) \quad (p^2 - 2\mu\tilde{\omega}_1\tilde{\omega}_2) \left(\frac{p^4}{2} + (\mu\tilde{\omega}_2 - \tilde{\omega}_1)(\tilde{\omega}_2 - \mu\tilde{\omega}_1)p^2 + 2\mu^2\tilde{\omega}_1^2\tilde{\omega}_2^2 \right) = 0.$$

296 For the first polynomial $p^2 - 2\mu\tilde{\omega}_1\tilde{\omega}_2$ in (3.9), there is always one positive root
 297 $\sqrt{2\mu\tilde{\omega}_1\tilde{\omega}_2}$ lying in the interval I_c , as $\sqrt{\tilde{\omega}_1\tilde{\omega}_2} \in [\tilde{\omega}_1, \tilde{\omega}_2]$. For the second polyno-
 298 mial in (3.9), it is exactly the fourth-order polynomial (3.8), and we will study in the
 299 following its roots according to the value of k_r .

300 Now, it remains to look at the optimized parameter p^* in the intervals I_l and I_r ,
 301 and compare the results with those of I_c . The situations in these two intervals are
 302 very similar, and thus it is sufficient to consider only one case, for instance, $p \in I_r$.
 303 In this case, the local maximum point $\tilde{\omega}_c = \frac{p}{\sqrt{2\mu}} \geq \tilde{\omega}_2$, and thus lies on the right of
 304 the interval $[\tilde{\omega}_1, \tilde{\omega}_2]$, as shown in Figure 3 on the right. In this case, we obtain once
 305 again from Lemma 3.3 that

$$306 \quad \max_{\tilde{\omega}_1 \leq \tilde{\omega} \leq \tilde{\omega}_2} \rho(\tilde{\omega}, p) = \max \{ \rho(\tilde{\omega}_1, p), \rho(\tilde{\omega}_2, p) \}.$$

307 When $p = \sqrt{2\mu}\tilde{\omega}_2$, we have $\tilde{\omega}_c = \tilde{\omega}_2$, and when p takes other values in I_r , $\tilde{\omega}_c$ moves
 308 away from $\tilde{\omega}_2$, as shown in Figure 3 on the right. Substituting $p = \sqrt{2\mu}\tilde{\omega}_2$ into (3.5)
 309 and using the fact that $k_r = \frac{\tilde{\omega}_2}{\tilde{\omega}_1}$, we obtain for the convergence factor at the endpoints
 310 $\tilde{\omega}_1$ and $\tilde{\omega}_2$

$$311 \quad \rho(\tilde{\omega}_1, \sqrt{2\mu}\tilde{\omega}_2) = R_{ext} := \sqrt{\frac{(\sqrt{2\mu}k_r - 1)^2 + 1}{(\sqrt{2k_r} + \sqrt{\mu})^2 + \mu} \frac{(\sqrt{2k_r} - \sqrt{\mu})^2 + \mu}{(\sqrt{2\mu}k_r + 1)^2 + 1}},$$

$$\rho(\tilde{\omega}_2, \sqrt{2\mu}\tilde{\omega}_2) = R_c.$$

312 In particular, when $k_r > h_1(\mu)$, we have $R_{ext} > R_c$. To find the optimized parameter
 313 p^* , we need to compare R_{ext} and R_c to determine the minimum of the convergence
 314 factor ρ . According to the value of k_r , we have the following three cases:

- 315 (i) if $k_r > h_2(\mu)$, then as $h_2(\mu) > h_1(\mu)$, we have $k_r > h_1(\mu)$, which implies
 316 $R_{ext} > R_c$. In this case, the value $\rho(\tilde{\omega}_1, p)$ increases as p increases in the inter-
 317 val I_r , so the convergence factor cannot be improved for $p \in I_r$, and the mini-
 318 mal convergence factor can only be obtained when $p \in I_c$. Furthermore, when
 319 $k_r > h_2(\mu)$, there is no positive root for the fourth-order polynomial (3.8),
 320 thus, only one positive root exists for the sixth-order polynomial (3.9), that
 321 is $p^* = \sqrt{2\mu\tilde{\omega}_1\tilde{\omega}_2} \in I_c$. Since the associated $\tilde{\omega}_c = \frac{p^*}{\sqrt{2\mu}} = \sqrt{\tilde{\omega}_1\tilde{\omega}_2}$, which falls
 322 in the interval $[\tilde{\omega}_1, \tilde{\omega}_2]$; then from Lemma 3.3, the maximum will be chosen
 323 either R_c or $\rho(\tilde{\omega}_1, p^*) = \rho(\tilde{\omega}_2, p^*)$. If $\rho(\tilde{\omega}_1, p^*) = \rho(\tilde{\omega}_2, p^*) \geq R_c$, then this
 324 minimizer p^* is unique for the min-max problem (P1). Otherwise, the max-
 325 imum is R_c , and the minimum of the min-max problem (P1) is also R_c . As
 326 R_c is independent of p , it can be attained for any p chosen in a closed interval
 327 around p^* ;
- 328 (ii) if $h_1(\mu) < k_r \leq h_2(\mu)$, we obtain once again $R_{ext} > R_c$. As discussed above
 329 in (i), the convergence factor in this case cannot be improved for $p \in I_r$,
 330 and the minimal value of the convergence factor will only be obtained when
 331 $p \in I_c$. Furthermore, the fourth-order polynomial (3.8) has one positive root
 332 in I_c if $k_r = h_2(\mu)$, and has two positive roots in I_c if $k_r < h_2(\mu)$. This
 333 implies that the sixth-order polynomial (3.9) has at least two roots in I_c , and

334 we have $\rho(\tilde{\omega}_1, p) = \rho(\tilde{\omega}_2, p) \leq R_c$. Therefore, R_c is the maximum value of ρ
 335 for $\tilde{\omega} \in [\tilde{\omega}_1, \tilde{\omega}_2]$. Then the minimum of the convergence factor is attained for
 336 any p chosen in a closed interval around p^* ;

337 (iii) if $k_r \leq h_1(\mu)$, we have $R_{ext} \leq R_c$. Therefore, we can find a unique value
 338 $p_r \in I_r$, $p_r \neq \sqrt{2\mu\tilde{\omega}_2}$ that satisfies $\rho(\tilde{\omega}_1, p_r) = \rho(\tilde{\omega}_2, p_r)$. This then results
 339 in the fourth-order polynomial (3.8), and we have in particular that $R_c >$
 340 $\rho(\tilde{\omega}_1, p_r) = \rho(\tilde{\omega}_2, p_r)$. Furthermore, for $p \in I_r$ and $p \neq \sqrt{2\mu\tilde{\omega}_2}$, $\tilde{\omega}_c \notin [\tilde{\omega}_1, \tilde{\omega}_2]$,
 341 then from Lemma 3.3, the maximum will only be chosen between $\rho(\tilde{\omega}_1, p)$ and
 342 $\rho(\tilde{\omega}_2, p)$, from which we find the minimizer of the min-max problem (P1). In
 343 particular, this minimum $\rho(\tilde{\omega}_1, p_r)$ beats the best convergence factor obtained
 344 for $p \in I_c$.

345 Based on the similarity of the two intervals I_r and I_l , we have respective results for
 346 $p \in I_l$. As all possible scenarios have been considered, this completes the proof. \square

347 **3.2. Local transmission parameter: Version II.** As discussed in Section 3.1,
 348 the choice (3.4) of the transmission parameter σ_j may not be optimal, as it only scales
 349 with respect to one diffusion coefficient. To improve it, we consider here a second
 350 choice of the local transmission parameters σ_j

$$351 \quad (3.10) \quad \sigma_1 = \sqrt{\nu_2}q, \quad \sigma_2 = \sqrt{\nu_1}q, \quad q > 0.$$

352 This choice now takes into account both diffusion coefficients ν_j but still with one free
 353 parameter q . Once again, the convergence of the optimized Schwarz algorithm (2.3)
 354 is guaranteed by Theorem 3.1 with q positive. For this choice of σ_j , the convergence
 355 factor (3.3) becomes

$$356 \quad (3.11) \quad \rho(\tilde{\omega}, q) = \sqrt{\frac{(q - \tilde{\omega})^2 + \tilde{\omega}^2}{(q + \mu\tilde{\omega})^2 + \mu^2\tilde{\omega}^2} \cdot \frac{(q - \tilde{\omega})^2 + \tilde{\omega}^2}{(q + \frac{1}{\mu}\tilde{\omega})^2 + \frac{1}{\mu^2}\tilde{\omega}^2}},$$

357 where $\mu = \sqrt{\frac{\nu_1}{\nu_2}}$ as before. The related min-max problem (P) becomes

$$358 \quad (P2) \quad \min_{q>0} \left(\max_{\tilde{\omega}_1 \leq \tilde{\omega} \leq \tilde{\omega}_2} \rho(\tilde{\omega}, q) \right),$$

359 which turns out to be much easier to analyze compared with the mix-max prob-
 360 lem (P1), and we can find a unique optimized transmission parameter p .

361 **THEOREM 3.6** (Optimized transmission parameter: Version II). *The unique op-*
 362 *timized transmission parameter q^* by solving the min-max problem (P2) is given by*
 363 $q^* = \sqrt{2\tilde{\omega}_1\tilde{\omega}_2}$.

364 *Proof.* The proof follows similar ideas in the proof of Lemma 3.2 and Lemma 3.3.
 365 More precisely, we first take the partial derivative of the convergence factor (3.11)
 366 with respect to the transmission parameter q and the frequency $\tilde{\omega}$ respectively,

$$367 \quad \text{sign} \left(\frac{\partial \rho}{\partial q} \right) = \text{sign}(q^2 - 2\tilde{\omega}^2), \quad \text{sign} \left(\frac{\partial \rho}{\partial \tilde{\omega}} \right) = \text{sign}(2\tilde{\omega}^2 - q^2).$$

368 From the partial derivative with respect to q and $\tilde{\omega}$, we observe that:

369 (i) increasing q will make the convergence factor (3.11) decrease when $q < \sqrt{2\tilde{\omega}_1}$,
 370 and decreasing q will make the convergence factor (3.11) decrease when $q >$
 371 $\sqrt{2\tilde{\omega}_2}$. Therefore, we can restrict the range of q to the interval $[\sqrt{2\tilde{\omega}_1}, \sqrt{2\tilde{\omega}_2}]$;

372 (ii) from the partial derivative with respect to the frequency $\tilde{\omega}$, the convergence
 373 factor $\rho(\tilde{\omega}, q)$ is decreasing for $\tilde{\omega} \in (\tilde{\omega}_1, \frac{q}{\sqrt{2}})$ and is increasing for $\tilde{\omega} \in (\frac{q}{\sqrt{2}}, \tilde{\omega}_2)$.

374 This implies that the maximum of the convergence factor $\rho(\tilde{\omega}, q)$ in the range
 375 $[\tilde{\omega}_1, \tilde{\omega}_2]$ is $\max\{\rho(\tilde{\omega}_1, q), \rho(\tilde{\omega}_2, q)\}$;

376 (iii) as for determining the minimum in the min-max problem (P2), we find that
 377 $\rho(\tilde{\omega}_1, q)$ is increasing, and $\rho(\tilde{\omega}_2, q)$ is decreasing for $q \in [\sqrt{2}\tilde{\omega}_1, \sqrt{2}\tilde{\omega}_2]$.

378 We can thus conclude that the convergence factor is minimized uniformly by equioscil-
 379 lation, when its value at ω_1 and ω_2 are equal, i.e., $\rho(\tilde{\omega}_1, q^*) = \rho(\tilde{\omega}_2, q^*)$. Solving this
 380 equation gives the unique optimized transmission parameter $q^* = \sqrt{2\tilde{\omega}_1\tilde{\omega}_2}$. \square

381 **3.3. Local transmission parameter: Version III.** In Section 3.2, we showed
 382 a choice (3.10) taking into account both two diffusion coefficients ν_j and found a
 383 unique optimized transmission parameter for the min-max problem (P2). However,
 384 we still have only one parameter to tune with this choice for both subdomains Q_1 and
 385 Q_2 . More generally, we can consider two transmission parameters,

$$386 \quad (3.12) \quad \sigma_1 = \sqrt{\nu_2 p}, \quad \sigma_2 = \sqrt{\nu_1 q}, \quad p, q > 0.$$

387 with two free parameters each for the subdomain. The convergence factor (3.3) for
 388 this choice becomes

$$389 \quad (3.13) \quad \rho(\tilde{\omega}, p, q) = \sqrt{\frac{(p - \tilde{\omega})^2 + \tilde{\omega}^2}{(p + \mu\tilde{\omega})^2 + \mu^2\tilde{\omega}^2} \cdot \frac{(q - \tilde{\omega})^2 + \tilde{\omega}^2}{(q + \frac{1}{\mu}\tilde{\omega})^2 + \frac{1}{\mu^2}\tilde{\omega}^2}}.$$

390 To guarantee convergence of the optimized Schwarz algorithm (2.3), we state next a
 391 sufficient condition for the parameters p and q based on Theorem 3.1.

392 **COROLLARY 3.7** (Sufficient condition). *Suppose that the transmission param-*
 393 *eters $p, q > 0$ satisfy*

$$394 \quad 0 < q \leq p \quad \text{if } \nu_1 < \nu_2, \quad 0 < p \leq q \quad \text{if } \nu_2 < \nu_1.$$

395 *Then, we have $\rho(\tilde{\omega}, p, q) < 1$ for all $\tilde{\omega} \in [\tilde{\omega}_1, \tilde{\omega}_2]$.*

396 The related min-max problem is

$$397 \quad (\text{P3}) \quad \min_{p, q > 0} \left(\max_{\tilde{\omega}_1 \leq \tilde{\omega} \leq \tilde{\omega}_2} \rho(\tilde{\omega}, p, q) \right).$$

398 In the following, we consider parameters p and q that satisfy the conditions in Corol-
 399 lary 3.7 to make the optimized Schwarz algorithm (2.3) converge. To optimize these
 400 two parameters, we follow once again similar steps as in the previous two sections,
 401 that is, we first restrict the range for the parameters (p, q) and locate possible values
 402 of the local maximum point $\tilde{\omega}$. Then, we analyze how these local maximum points be-
 403 have when the parameters (p, q) vary. The following result provides the order between
 404 p and q in terms of the diffusion coefficient ratio μ .

405 **LEMMA 3.8** (Order of p and q). *If $\mu > 1$, the min-max problem (P3) is equivalent*
 406 *to*

$$407 \quad \min_{0 < p \leq q} \left(\max_{\tilde{\omega}_1 \leq \tilde{\omega} \leq \tilde{\omega}_2} \rho(\tilde{\omega}, p, q) \right).$$

408 *If $\mu < 1$, the min-max problem (P3) is equivalent to*

$$409 \quad \min_{0 < q \leq p} \left(\max_{\tilde{\omega}_1 \leq \tilde{\omega} \leq \tilde{\omega}_2} \rho(\tilde{\omega}, p, q) \right).$$

410 *Proof.* Generally, we can consider solving the min-max problem in the case $\mu > 1$.
 411 The other case $\mu < 1$ turns to the case $\mu > 1$ by interchanging p and q and replacing
 412 μ by $1/\mu$ in (3.13). Thus, we assume that $\mu > 1$ and $p > q$. The convergence factor
 413 is given by (3.13). Interchanging the values of p and q in (3.13), this becomes

$$414 \quad \rho(\tilde{\omega}, q, p) = \sqrt{\frac{(q - \tilde{\omega})^2 + \tilde{\omega}^2}{(q + \mu\tilde{\omega})^2 + \mu^2\tilde{\omega}^2} \cdot \frac{(p - \tilde{\omega})^2 + \tilde{\omega}^2}{(p + \frac{1}{\mu}\tilde{\omega})^2 + \frac{1}{\mu^2}\tilde{\omega}^2}}.$$

415 In particular, we have

$$416 \quad \text{sign}(\rho(\tilde{\omega}, p, q)^2 - \rho(\tilde{\omega}, q, p)^2) = \text{sign}((\mu - 1)(p - q)).$$

417 In the case $\mu > 1$ and $p > q$, we have $\rho(\tilde{\omega}, p, q) > \rho(\tilde{\omega}, q, p)$, meaning that the
 418 convergence factor ρ is uniformly improved by interchanging p and q . Therefore,
 419 when $\mu > 1$, it is sufficient to consider the parameters $p \leq q$. \square

420 From now on, we assume that $\mu > 1$ and hence $0 < p \leq q$. Then, the conditions
 421 in Corollary 3.7 are well satisfied. In this case, we find a similar result as Lemma 3.2.

422 LEMMA 3.9 (Restrict p and q). *When $\mu > 1$, we can restrict the range of the*
 423 *parameters p and q to the intervals*

$$424 \quad \begin{aligned} p &\in [\tilde{\omega}_1(\sqrt{\mu^2 + 1} - (\mu - 1)), \tilde{\omega}_2(\sqrt{\mu^2 + 1} - (\mu - 1))], \\ q &\in [\tilde{\omega}_1 \frac{\sqrt{\mu^2 + 1} + (\mu - 1)}{\mu}, \tilde{\omega}_2 \frac{\sqrt{\mu^2 + 1} + (\mu - 1)}{\mu}]. \end{aligned}$$

425 *Proof.* Taking a partial derivative of the convergence factor (3.13) with respect
 426 to the transmission parameters p and q , we find

$$\begin{aligned} \text{sign} \left(\frac{\partial \rho}{\partial p} \right) &= \text{sign} (p^2 + 2p(\mu - 1)\tilde{\omega} - 2\mu\tilde{\omega}^2) \\ &= \begin{cases} \text{positive,} & \text{if } p > \tilde{\omega}(\sqrt{\mu^2 + 1} - (\mu - 1)), \\ \text{negative,} & \text{if } p < \tilde{\omega}(\sqrt{\mu^2 + 1} - (\mu - 1)). \end{cases} \\ 427 \quad \text{sign} \left(\frac{\partial \rho}{\partial q} \right) &= \text{sign} (\mu q^2 - 2q(\mu - 1)\tilde{\omega} - 2\tilde{\omega}^2) \\ &= \begin{cases} \text{positive,} & \text{if } q > \tilde{\omega} \frac{\sqrt{\mu^2 + 1} + (\mu - 1)}{\mu}, \\ \text{negative,} & \text{if } q < \tilde{\omega} \frac{\sqrt{\mu^2 + 1} + (\mu - 1)}{\mu}. \end{cases} \end{aligned}$$

428 Therefore, when $p < \tilde{\omega}_1(\sqrt{\mu^2 + 1} - (\mu - 1))$, increasing p improves uniformly the
 429 convergence factor ρ , while when $p > \tilde{\omega}_2(\sqrt{\mu^2 + 1} - (\mu - 1))$, decreasing p will improve
 430 uniformly the convergence factor ρ . Similar arguments hold for the transmission
 431 parameter q . Therefore, the two restriction intervals follow. \square

432 From the range of p and q , we observe that $\frac{pq}{2}$ is actually in the range of $[\tilde{\omega}_1^2, \tilde{\omega}_2^2]$.
 433 Furthermore, once we restrict the transmission parameters p and q , we can find the
 434 local maxima of $\tilde{\omega}$ as in Lemma 3.3. Note also that in practice for common choices
 435 of $\tilde{\omega}_j$, where $\tilde{\omega}_2$ is much larger than $\tilde{\omega}_1$, we numerically find that the convergence
 436 factor ρ behaves as in Figure 4 when the optimized parameters are obtained. Thus,
 437 we consider in the following such convergence behavior and determine the associated
 438 optimized parameter pair (p, q) .

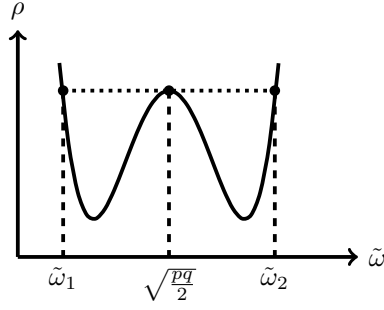


FIG. 4. Illustration of the convergence factor with respect to $\tilde{\omega}$, when the optimized p and q are obtained.

439 LEMMA 3.10 (Local maxima of $\tilde{\omega}$). For $\tilde{\omega} \in [\tilde{\omega}_1, \tilde{\omega}_2]$, the maximum of the con-
440 vergence factor is

$$441 \quad (3.14) \quad \max_{\tilde{\omega}_1 \leq \tilde{\omega} \leq \tilde{\omega}_2} \rho(\tilde{\omega}, p, q) = \max \left\{ \rho(\tilde{\omega}_1, p, q), \rho\left(\sqrt{\frac{pq}{2}}, p, q\right), \rho(\tilde{\omega}_2, p, q) \right\}.$$

442 *Proof.* Taking a partial derivative of (3.13) with respect to $\tilde{\omega}$, we get

$$443 \quad (3.15) \quad \text{sign} \left(\frac{\partial \rho}{\partial \tilde{\omega}} \right) = \text{sign} \left((2\tilde{\omega}^2 - pq) \times \right. \\ \left. \left(\tilde{\omega}^2 + \frac{(\mu - 1)(\gamma\mu - 1) - \sqrt{(\mu^2 + 1)(\gamma^2\mu^2 + 1)}}{2\mu} p\tilde{\omega} + \frac{\gamma p^2}{2} \right) \right),$$

444 where we introduced the ratio $\gamma := \frac{q}{p}$. When the first polynomial of $\tilde{\omega}$ in (3.15)
445 equals zero, i.e., $2\tilde{\omega}^2 - pq = 0$, we obtain that $\tilde{\omega} = \sqrt{\frac{pq}{2}}$. To study whether this value
446 is a local maximum point for $\tilde{\omega} \in [\tilde{\omega}_1, \tilde{\omega}_2]$, we need to know the sign of the second
447 polynomial in (3.15) near the point $\tilde{\omega} = \sqrt{\frac{pq}{2}}$. Using the ratio γ , we have $\tilde{\omega}^2 = \frac{\gamma p^2}{2}$.
448 Substituting this into the second polynomial of $\tilde{\omega}$ in (3.15), we find

$$449 \quad (3.16) \quad \gamma p^2 + \sqrt{\frac{\gamma(\mu - 1)(\gamma\mu - 1) - \sqrt{(\mu^2 + 1)(\gamma^2\mu^2 + 1)}}{2\mu}} p^2.$$

450 Supposing that (3.16) is nonnegative, we get

$$451 \quad \frac{(\mu - 1)(\gamma\mu - 1) - \sqrt{(\mu^2 + 1)(\gamma^2\mu^2 + 1)}}{2\mu} \geq -\sqrt{2\gamma}.$$

452 We can then bound the second polynomial in (3.15) by

$$453 \quad \tilde{\omega}^2 + \frac{(\mu - 1)(\gamma\mu - 1) - \sqrt{(\mu^2 + 1)(\gamma^2\mu^2 + 1)}}{2\mu} p\tilde{\omega} + \frac{\gamma p^2}{2} \geq \\ \tilde{\omega}^2 - \sqrt{2\gamma} p\tilde{\omega} + \frac{\gamma p^2}{2} = \left(\tilde{\omega} - \frac{\sqrt{2\gamma} p}{2} \right)^2 \geq 0.$$

454 This implies that the second polynomial in (3.15) is nonnegative, and the sign of the
455 partial derivative only depends on the first polynomial in (3.15), that is, $\rho(\tilde{\omega}, p, q)$
456 is decreasing for $\tilde{\omega} \in [\tilde{\omega}_1, \sqrt{\frac{pq}{2}}]$ and is increasing for $\tilde{\omega} \in [\sqrt{\frac{pq}{2}}, \tilde{\omega}_2]$. This contradicts the

457 fact that the convergence ρ behaves as in Figure 4. Therefore, the equation (3.16) is
 458 negative, and the second polynomial in (3.15) is also negative when $\tilde{\omega}^2 = \frac{pq}{2}$. For this
 459 reason, the convergence factor ρ has a local maximum in $\tilde{\omega}$ at $\sqrt{\frac{pq}{2}}$. According to the
 460 range of the transmission parameters p and q , we have $\sqrt{\frac{pq}{2}} \in [\tilde{\omega}_1, \tilde{\omega}_2]$. Therefore, the
 461 maximum value of the convergence factor $\rho(\tilde{\omega}, p, q)$ for $\tilde{\omega} \in [\tilde{\omega}_1, \tilde{\omega}_2]$ is given by (3.14). \square

462 With the help of Lemma 3.9 and Lemma 3.10, we obtain a similar result as
 463 Theorem 3.4 and Theorem 3.6 that the optimized transmission parameter pair (p^*, q^*)
 464 can be obtained by an equioscillation of these three local maxima.

465 **THEOREM 3.11** (Optimized transmission parameters: Version III). *When $\mu > 1$,
 466 the unique minimizer pair (p^*, q^*) of Problem (P3) is the solution of the system of
 467 the two equations*

$$468 \quad \rho(\tilde{\omega}_1, p^*, q^*) = \rho(\tilde{\omega}_2, p^*, q^*), \quad \rho(\tilde{\omega}_1, p^*, q^*) = \rho(\sqrt{\tilde{\omega}_1 \tilde{\omega}_2}, p^*, q^*).$$

469 *Proof.* According to the equioscillation principle, we need to have at the end-
 470 points of the frequency $\tilde{\omega}$ that $\rho(\tilde{\omega}_1, p, q) = \rho(\tilde{\omega}_2, p, q)$ to acquire the minimum of the
 471 convergence factor ρ . After some algebraic simplification, we obtain $pq = 2\tilde{\omega}_1 \tilde{\omega}_2$. This
 472 then enables us to reduce the range of the parameter to $p \in I_p := [\tilde{\omega}_1(\sqrt{\mu^2 + 1} - (\mu -$
 473 $1)), \sqrt{2\tilde{\omega}_1 \tilde{\omega}_2}]$, and the min-max problem (P3) becomes

$$474 \quad \min_{p \in I_p} \left(\max\{R_1(p), R_c(p)\} \right), \quad R_1(p) := \rho(\tilde{\omega}_1, p, \frac{2\tilde{\omega}_1 \tilde{\omega}_2}{p}), \quad R_c(p) := \rho(\sqrt{\tilde{\omega}_1 \tilde{\omega}_2}, p, \frac{2\tilde{\omega}_1 \tilde{\omega}_2}{p}).$$

475 Using once again the equioscillation principle, the optimized parameters p^* can be
 476 found when $R_1(p) = R_c(p)$ for $p \in I_p$, which can be reduced to the equation

$$477 \quad (3.17) \quad \frac{(p - \tilde{\omega}_1)^2 + \tilde{\omega}_1^2}{(p + \mu\tilde{\omega}_1)^2 + \mu^2\tilde{\omega}_1^2} \cdot \frac{(p - \tilde{\omega}_2)^2 + \tilde{\omega}_2^2}{(p + \mu\tilde{\omega}_2)^2 + \mu^2\tilde{\omega}_2^2} = \left(\frac{(p - \sqrt{\tilde{\omega}_1 \tilde{\omega}_2})^2 + \tilde{\omega}_1 \tilde{\omega}_2}{(p + \mu\sqrt{\tilde{\omega}_1 \tilde{\omega}_2})^2 + \mu^2\tilde{\omega}_1 \tilde{\omega}_2} \right)^2.$$

478 Solving this polynomial of p , we can identify the optimized transmission parameters.
 479 Note that there exist closed forms for the roots of this polynomial. Among all, we can
 480 list three simple solutions, that are 0 and $\pm i\sqrt{2\mu\tilde{\omega}_1 \tilde{\omega}_2}$, the other roots are much more
 481 complicated. In practice, when the time step Δt is small, the frequency $\tilde{\omega}_2 = \sqrt{\frac{\pi}{2\Delta t}}$
 482 is much greater than $\tilde{\omega}_1 = \sqrt{\frac{\pi}{4T}}$. In this case, we can use asymptotic analysis and
 483 find an approximate solution $p^* \approx \frac{2\mu}{\mu-1}\tilde{\omega}_1$, which lies in the interval I_p . Overall, for
 484 all the roots, we find one unique real root $p^* \in I_p$, and use once again the fact that
 485 $pq = 2\tilde{\omega}_1 \tilde{\omega}_2$ to find q^* , and this completes the proof. \square

486 *Remark 3.12.* To avoid complex and expensive calculation, we can show numer-
 487 ically the graph of (3.17) in Figure 5 where $p \in I_p$ with a set of $(\tilde{\omega}_1, \tilde{\omega}_2, \mu)$. It can
 488 be seen that there exists a unique root in (3.17) for $p \in I_p$. Note that the behavior
 489 illustrated in Figure 5 remains similar for all our numerical experiments with different
 490 sets of $(\tilde{\omega}_1, \tilde{\omega}_2, \mu)$.

491 **4. Asymptotic analysis.** We now analyze the asymptotic convergence behavior
 492 using the three versions of local transmission parameters presented in Section 3.

493 **4.1. Asymptotic behavior for large diffusion ratio.** When the heat diffu-
 494 sion coefficient ratio is large, the thermal conductivities between two materials are
 495 very different. In this case, we can analyze the asymptotic convergence behavior of
 496 the optimized Schwarz algorithm. Recall that the diffusion coefficient ratio is given
 497 by $\mu^2 = \frac{\nu_1}{\nu_2}$. As explained in Section 3, we only consider the case $\mu > 1$.

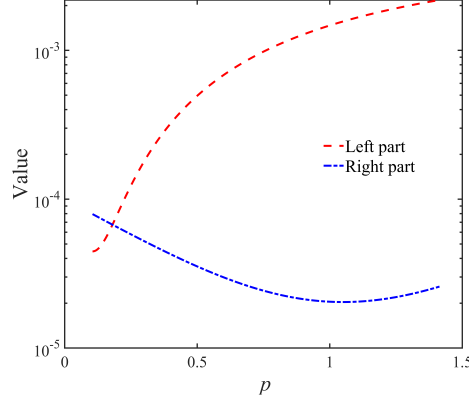


FIG. 5. Illustration of the left and rights part in (3.17) for $p \in I_p$.

498 THEOREM 4.1 (Asymptotics for large μ). For given Δt and T , when $\mu \rightarrow \infty$,
 499 the asymptotic behavior of each convergence factor using optimized parameters is as
 500 follows:

501 Version I:

$$502 \quad (4.1) \quad \max_{\tilde{\omega}_1 \leq \tilde{\omega} \leq \tilde{\omega}_2} \rho(\tilde{\omega}, p^*) = \sqrt{\frac{\tilde{\omega}_1 + \tilde{\omega}_2 - \sqrt{2\tilde{\omega}_1\tilde{\omega}_2}}{\tilde{\omega}_1 + \tilde{\omega}_2 + \sqrt{2\tilde{\omega}_1\tilde{\omega}_2}}} + O\left(\frac{1}{\mu}\right).$$

503 Version II:

$$504 \quad (4.2) \quad \max_{\tilde{\omega}_1 \leq \tilde{\omega} \leq \tilde{\omega}_2} \rho(\tilde{\omega}, q^*) = \frac{\tilde{\omega}_1 - \sqrt{2\tilde{\omega}_1\tilde{\omega}_2} + \tilde{\omega}_2}{\sqrt{\tilde{\omega}_1\tilde{\omega}_2}} \frac{1}{\mu} + O\left(\frac{1}{\mu^2}\right).$$

505 Version III:

$$506 \quad (4.3) \quad \max_{\tilde{\omega}_1 \leq \tilde{\omega} \leq \tilde{\omega}_1} \rho(\tilde{\omega}, p^*, q^*) = \frac{\sqrt{((p_0^* - \tilde{\omega}_1)^2 + \tilde{\omega}_1^2)((q_0^* - \tilde{\omega}_1)^2 + \tilde{\omega}_1^2)}}{\sqrt{2q_0^*\tilde{\omega}_1}} \frac{1}{\mu} + O\left(\frac{1}{\mu^2}\right).$$

507 *Proof.* For Version I, when μ is large enough, we are in the case (iii) of Theorem 3.5
 508 since $k_r < h_1(\mu)$. Then, as discussed in (iii) of Theorem 3.5, the minimum is attained
 509 with two distinct optimized parameters p_l^* and p_r^* , which are two positive roots of the
 510 fourth-order polynomial (3.8). When the ratio μ goes to infinity, the two parameters
 511 have the expansions

$$512 \quad p_l^* = \sqrt{2\tilde{\omega}_1\tilde{\omega}_2} + \frac{\tilde{\omega}_1^2 + \tilde{\omega}_2^2}{\sqrt{2\tilde{\omega}_1\tilde{\omega}_2}} \frac{1}{\mu} + O\left(\frac{1}{\mu^2}\right), \quad p_r^* = \sqrt{2\tilde{\omega}_1\tilde{\omega}_2}\mu - \frac{\tilde{\omega}_1^2 + \tilde{\omega}_2^2}{\sqrt{2\tilde{\omega}_1\tilde{\omega}_2}} + O\left(\frac{1}{\mu}\right).$$

513 Evaluating then $\rho(\tilde{\omega}_1, p_l^*)$ (or p_r^*) and expanding for $\mu \rightarrow \infty$, we find the asymptotic
 514 convergence behavior (4.1).

515 For Version II, the optimized parameter $q^* = \sqrt{2\tilde{\omega}_1\tilde{\omega}_2}$ is independent of μ as
 516 shown in Theorem 3.6. Hence, a straightforward expansion of the convergence factor
 517 (3.11) for $\mu \rightarrow \infty$ gives the asymptotic behavior (4.2).

518 With Theorem 3.11, the optimized parameters of Version III can be obtained by

519 solving the equation (3.17). In the limit case, we have

$$520 \quad p_0^* := \lim_{\mu \rightarrow \infty} p^* = \frac{(\sqrt{\tilde{\omega}_1} + \sqrt{\tilde{\omega}_2})^2 - \sqrt{(\sqrt{\tilde{\omega}_1} + \sqrt{\tilde{\omega}_2})^4 - 8\tilde{\omega}_1\tilde{\omega}_2}}{2},$$

$$q_0^* := \lim_{\mu \rightarrow \infty} q^* = \frac{(\sqrt{\tilde{\omega}_1} + \sqrt{\tilde{\omega}_2})^2 + \sqrt{(\sqrt{\tilde{\omega}_1} + \sqrt{\tilde{\omega}_2})^4 - 8\tilde{\omega}_1\tilde{\omega}_2}}{2}.$$

521 Using then Theorem 3.11, we evaluate $\rho(\tilde{\omega}_1, p_0^*, q_0^*)$ and expand for $\mu \rightarrow \infty$, which
522 gives the asymptotic behavior (4.3). \square

523 From the asymptotic convergence behavior given in Theorem 4.1, we see that
524 the convergence factor of Version I behaves as a constant, which depends only on
525 the time step Δt and the time interval length T , whereas the convergence factors of
526 Versions II and III approach zero when $\mu \rightarrow \infty$. In other words, when the material
527 conductivity properties vary significantly between different materials, the convergence
528 of the Schwarz iteration (2.2) with optimized parameters from Versions II and III is
529 much better with Version I. This is also confirmed by our numerical experiments in
530 Table 1.

531 **4.2. Asymptotic behavior for small time step.** Recall that $\tilde{\omega}_2 = \sqrt{\frac{\pi}{2\Delta t}}$, and
532 thus the frequency interval length $[\tilde{\omega}_1, \tilde{\omega}_2]$ depends on the time step Δt . When Δt
533 goes to zero, more high frequencies will be covered, and we can analyze the asymptotic
534 convergence behavior of the optimized Schwarz algorithm using our three versions of
535 optimized parameters.

536 **THEOREM 4.2** (Asymptotics for small Δt). *For given T and $\mu > 1$, when $\Delta t \rightarrow$
537 0 , the asymptotic behavior of each convergence factor using optimized parameters is
538 as follows:*

539 *Version I:*

$$540 \quad (4.4) \quad \max_{\tilde{\omega}_1 \leq \tilde{\omega} \leq \tilde{\omega}_2} \rho(\tilde{\omega}, p^*) = 1 - 2 \left(\sqrt{\mu} + \frac{1}{\sqrt{\mu}} \right) \sqrt{\frac{\tilde{\omega}_1}{\sqrt{2\pi}}} \Delta t^{\frac{1}{4}} + O(\Delta t^{\frac{1}{2}}).$$

541 *Version II:*

$$542 \quad (4.5) \quad \max_{\tilde{\omega}_1 \leq \tilde{\omega} \leq \tilde{\omega}_2} \rho(\tilde{\omega}, q^*) = 1 - \frac{(\mu + 1)^2}{\mu} \sqrt{\frac{\tilde{\omega}_1}{\sqrt{2\pi}}} \Delta t^{\frac{1}{4}} + O(\Delta t^{\frac{1}{2}}).$$

543 *Version III:*

$$544 \quad (4.6) \quad \max_{\tilde{\omega}_1 \leq \tilde{\omega} \leq \tilde{\omega}_2} \rho(\tilde{\omega}, p^*, q^*) = \frac{1}{\mu} - \frac{2(\mu + 1)}{\mu(\mu - 1)} \sqrt{\frac{\tilde{\omega}_1}{\sqrt{\frac{\pi}{2}}}} \Delta t^{\frac{1}{4}} + O(\Delta t^{\frac{1}{2}}).$$

545 *Proof.* For Version I, when the time step Δt goes to zero, we are in the case (i)
546 of Theorem 3.5 or Theorem 3.4, depending on the value of μ . In both cases, we have
547 $p^* = \sqrt{2\mu\tilde{\omega}_1\tilde{\omega}_2} = \sqrt{\sqrt{2\pi}\mu\tilde{\omega}_1}\Delta t^{-\frac{1}{4}}$. Substituting this into $\rho(\tilde{\omega}_1, p^*)$ and expanding
548 for $\Delta t \rightarrow 0$ gives the asymptotic result (4.4). Furthermore, if $1 < \mu \leq 2 + \sqrt{3}$,
549 Theorem 3.4 shows that the optimized parameter p^* is unique. In the case when
550 $\mu > 2 + \sqrt{3}$, R_c defined in Theorem 3.5 is a constant strictly smaller than 1, and the
551 asymptotic result (4.4) approaches 1 as $\Delta t \rightarrow 0$. Therefore, part (i) of Theorem 3.5
552 also guarantees the uniqueness of the optimized parameter p^* .

553 Similarly, for Version II, Theorem 3.6 shows that the optimized parameter is
 554 $q^* = \sqrt{2\tilde{\omega}_1\tilde{\omega}_2} = \sqrt{\sqrt{2\pi}\tilde{\omega}_1}\Delta t^{-\frac{1}{4}}$. Substituting this into $\rho(\tilde{\omega}_1, q^*)$ and expanding for
 555 $\Delta t \rightarrow 0$ gives the asymptotic result (4.5).

556 For Version III, we make the Ansatz $p^* = A\Delta t^\alpha + B\Delta t^\beta$ with $\alpha < \beta \in \mathbb{R}$.
 557 Substituting this Ansatz into (3.17) and expanding for small Δt , we obtain $\alpha = 0$,
 558 $\beta = \frac{1}{4}$ by matching the two dominant terms and find the optimized parameter p^* as

$$559 \quad p^* = \frac{2\mu\tilde{\omega}_1}{\mu-1} - \frac{4\mu\tilde{\omega}_1^{\frac{3}{2}}(\mu^2+1)}{\left(\frac{\pi}{2}\right)^{\frac{1}{4}}(\mu-1)^3}\Delta t^{\frac{1}{4}}.$$

560 The optimized parameter q^* is then obtained from $p^*q^* = 2\tilde{\omega}_1\tilde{\omega}_2$ as

$$561 \quad q^* = \frac{\sqrt{2\pi}(\mu-1)}{2\mu}\Delta t^{-\frac{1}{2}} + \frac{\sqrt{2\tilde{\omega}_1^{\frac{1}{2}}(\mu^2+1)}}{\mu(\mu-1)}(2\pi)^{\frac{1}{4}}\Delta t^{-\frac{1}{4}}.$$

562 Finally, substituting p^*, q^* into $\rho(\tilde{\omega}_1, p^*, q^*)$ and expanding for $\Delta t \rightarrow 0$ gives the
 563 asymptotic result (4.6). \square

564 From the asymptotic behavior given in Theorem 4.2, we first observe that the
 565 convergence factor of Versions I and II approaches 1 when $\Delta t \rightarrow 0$, whereas the con-
 566 vergence factor of Version III approaches $1/\mu$. Therefore, good convergence behavior
 567 can still be guaranteed using the optimized parameters from Version III for small time
 568 step sizes, in particular when the diffusion coefficient ratio μ is large. This observation
 569 is confirmed by our numerical experiments (see Figure 8). However, the asymptotic
 570 expansions for Version III cannot be used when $\mu = 1$, whereas we can recover the op-
 571 timized parameters in [9, Section 3] for homogeneous diffusion coefficients by setting
 572 $\mu = 1$ in Versions I and II. Hence, these two versions can provide useful insight into the
 573 optimized parameters and asymptotic behavior when the material is homogeneous.

574 **5. Numerical Experiments.** We now show some numerical experiments to
 575 compare the performance of the three local approximations of the optimal operator σ_j
 576 discussed in Section 3. For our numerical tests, we consider solving the problem (2.1)
 577 in a one-dimensional space domain $\Omega = (0, 1)$ and for a fixed final time $T = 5$.
 578 Furthermore, we take a source term $f = 0$, a constant initial condition $u_0 = 20$ and a
 579 homogeneous Dirichlet boundary condition $g = 0$. The space domain Ω is decomposed
 580 into two nonoverlapping subdomains $\Omega_1 = (0, \frac{1}{2})$ and $\Omega_2 = (\frac{1}{2}, 1)$. In all numerical
 581 experiments, the heat diffusion coefficients are $\nu_1 = 1$ and $\nu_2 = \frac{1}{\mu^2}$, where the ratio
 582 $\mu^2 = \frac{\nu_1}{\nu_2}$ is always chosen to be greater than 1. We use a finite element discretization
 583 in space with a uniform mesh size Δx , and a backward Euler discretization in time
 584 with a constant time step Δt . In the Schwarz iteration, we use the l^∞ error

$$585 \quad e^n := \|\mathbf{U} - \mathbf{u}^n\|_\infty,$$

586 where \mathbf{U} is the discrete global solution of the problem (2.1) and \mathbf{u}^n is the combined
 587 solution of the subdomains at iteration n .

588 **5.1. Impact of the ratio μ .** We first test the impact of the heat diffusion
 589 coefficient ratio μ . For a given mesh size $\Delta x = 1/40$ and a time step $\Delta t = 1/40$, we
 590 show in Figure 6 the convergence behavior of the three local transmission conditions
 591 for the two different ratios $\frac{\nu_1}{\nu_2} = [10, 10^2]$.

592 We observe that the convergence behavior of Versions II and III is slightly better
 593 than that of Version I in the case $\mu^2 = 10$, as shown in Figure 6 on the left. However,

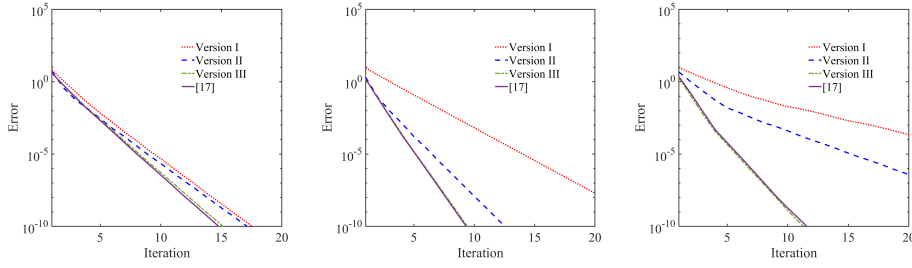


FIG. 6. Convergence behavior of the three local transmission conditions and the one from [17] with a mesh size $\Delta x = \frac{1}{40}$. Left: $\frac{\nu_1}{\nu_2} = 10$ and $\Delta t = \frac{1}{40}$. Middle: $\frac{\nu_1}{\nu_2} = 10^2$ and $\Delta t = \frac{1}{40}$. Right: $\nu_1 = 10^{-1}$, $\frac{\nu_1}{\nu_2} = 10^2$, and $\Delta t = \frac{1}{160}$.

TABLE 1
Number of iterations to reach a tolerance of 10^{-8} for four diffusion coefficient ratios $\frac{\nu_1}{\nu_2}$.

$\mu^2 = \frac{\nu_1}{\nu_2}$	Version I	Version II	Version III
10^1	15	14	13
10^2	21	11	8
10^3	39	9	6
10^4	169	9	6

594 for the ratio $\mu^2 = 10^2$, we observe in Figure 6 in the middle that the performance of
 595 Version II and III becomes much better, while Version I becomes less efficient. As ex-
 596 pected, the local transmission conditions Version II and Version III are appropriately
 597 scaled with respect to both diffusion coefficients ν_1 and ν_2 , and thus perform better;
 598 but Version I is only scaled with respect to one diffusion coefficient ν_2 , and thus is
 599 less robust when the ratio is changed. Overall, the performance of Version III is the
 600 best for the two cases tested.

601 We also show in Figure 6 a comparison of the convergence for our three versions
 602 with the optimized parameters given in [17, Theorem 4.6]. We see that the conver-
 603 gence behavior of Version III is very similar to the one with parameters from [17,
 604 Theorem 4.6]. The slight difference between them results from the estimate of the
 605 minimum frequency ω_{\min} : the authors in [17] used the Fourier transform in time to
 606 analyze the convergence and $\frac{\pi}{T}$ as the minimum Fourier frequency, while we use here
 607 the Laplace transform with the minimum Laplace frequency $\frac{\pi}{2T}$, which covers more
 608 low frequencies. Hence, our method has a slightly better performance when low fre-
 609 quencies are present in the heat diffusion, as illustrated on the right in Figure 6 for
 610 diffusion coefficients $\nu_1 = 0.1$ and $\nu_2 = 0.001$.

611 In Figure 7, we show the corresponding theoretical convergence factor ρ as a
 612 function of the frequency $\tilde{\omega}$ for our three versions. We see that the maximum over
 613 all $\tilde{\omega}$ is the smallest for Version III, and the largest for Version I, Version II being in
 614 between, which corresponds well to the numerical performance in Figure 6.

615 To get further insights into the impact of the ratio of the diffusion coefficients,
 616 we keep the mesh size $\Delta x = 1/40$ and the time step $\Delta t = 1/40$ fixed and vary the
 617 diffusion coefficients ratio μ^2 . Table 1 shows the number of iterations needed to reach
 618 a tolerance of 10^{-8} for the three versions when the diffusion coefficient ratio increases.
 619 We clearly see that the convergence behavior of Versions II and III is better than that
 620 of Version I. In particular, as Version I is only scaled with respect to ν_2 for both local

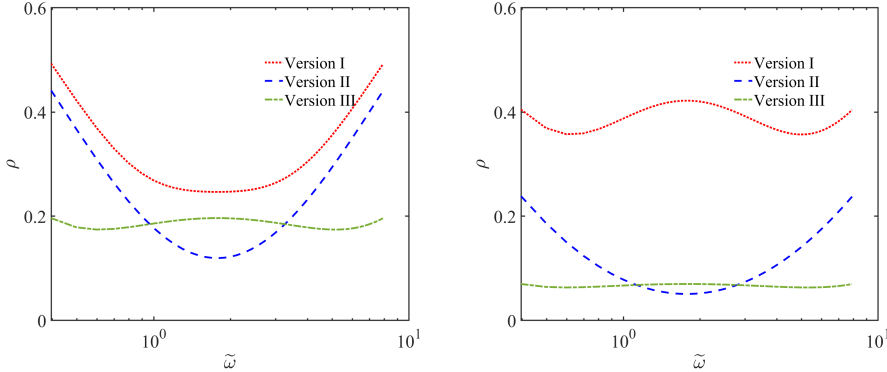


FIG. 7. Comparison of the convergence factor ρ with respect to the frequency $\tilde{\omega}$ for all three versions. Left: $\frac{\nu_1}{\nu_2} = 10$. Right: $\frac{\nu_1}{\nu_2} = 10^2$.

621 transmission parameters, that is, $\sigma_1 = \sigma_2 = \sqrt{\nu_2 p}$, when the ratio μ increases, they
 622 cannot take into account this change accordingly in each subdomain, and become
 623 much worse for large ratios. In contrast, both Versions II and III are scaled with
 624 respect to the two diffusion coefficients ν_1 and ν_2 , and are thus able to handle much
 625 better changing diffusion coefficient ratios. They become even much more efficient
 626 and robust for a large coefficient ratio μ . Among all, Version III outperforms the
 627 others for all tested cases in Table 1.

628 **5.2. Influence of the time step Δt .** Next, we test the impact of the time step
 629 Δt , which will influence the high frequency value $\omega_{\max} = \pi/\Delta t$, thus changing the
 630 range of the frequency ω . We keep the same mesh size $\Delta x = 1/40$ and consider two
 631 different diffusion coefficient ratios $\frac{\nu_1}{\nu_2} = 10$ and $\frac{\nu_1}{\nu_2} = 10^3$. The convergence behavior
 632 for four different time steps $\Delta t = [\frac{1}{20}, \frac{1}{40}, \frac{1}{80}, \frac{1}{160}]$ is shown in Figure 8 for both diffusion
 633 coefficient ratios. We see on the left and in the middle that convergence of Versions
 634 I and II deteriorates when the time step Δt decreases, whereas the performance of
 635 Version III on the right varies very little when decreasing the time step, especially
 636 for large diffusion coefficient ratios. Among all the tested cases, the convergence of
 637 Version III is more stable.

638 **5.3. Influence of the mesh size Δx .** In a similar way, we test now the impact
 639 of the mesh size Δx in the case of a relatively small diffusion coefficient ratio $\frac{\nu_1}{\nu_2} = 10$
 640 and a large diffusion coefficient ratio $\frac{\nu_1}{\nu_2} = 10^3$, and keep the time step $\Delta t = 1/40$
 641 fixed. We show in Figure 9 the convergence behavior for the three different mesh sizes
 642 $\Delta x = [\frac{1}{20}, \frac{1}{40}, \frac{1}{80}]$. Compared with the impact of the time steps, the impact of the mesh
 643 size for all three versions is relatively small, especially for the diffusion ratio $\frac{\nu_1}{\nu_2} = 10$
 644 as shown in Figure 9 on the top. As for the ratio $\frac{\nu_1}{\nu_2} = 10^3$, we observe in Figure 9 at
 645 the bottom that the performance of all three versions is slightly improved for small
 646 mesh size in contrast to when Δt becomes small; and once again, the convergence of
 647 Version III is more stable among all tested cases as shown in Figure 9 on the right.

648 **5.4. Application to thermal protection systems simulation.** To generalize
 649 our studies to practical applications, we now provide a numerical investigation of the
 650 thermal protection structure presented in Figure 1 in a one-dimensional framework.
 651 Based on the three-layer structure of the materials, we consider a natural asymmetric

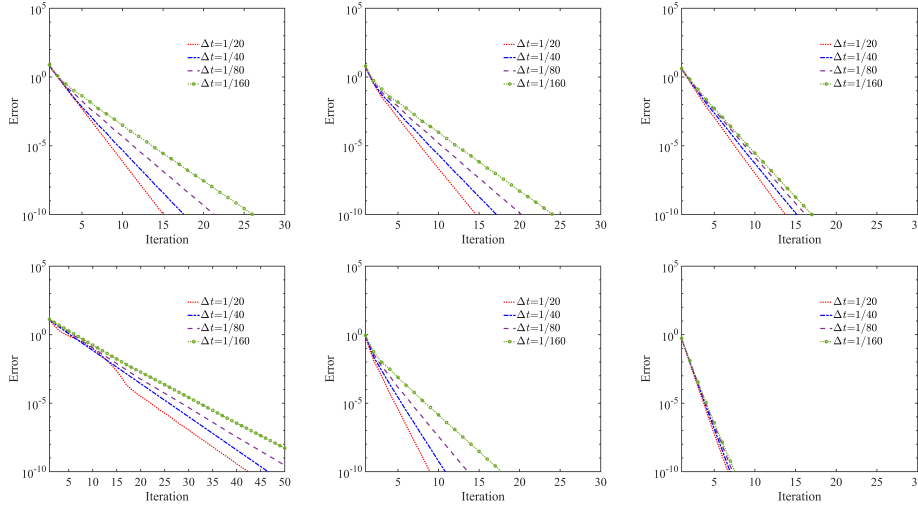


FIG. 8. Convergence behavior of the three local transmission conditions with a given mesh size $\Delta x = \frac{1}{40}$ and four different time steps $\Delta t = [\frac{1}{20}, \frac{1}{40}, \frac{1}{80}, \frac{1}{160}]$. Top: $\frac{\nu_1}{\nu_2} = 10$. Bottom: $\frac{\nu_1}{\nu_2} = 10^3$. Left: Version I. Middle: Version II. Right: Version III.

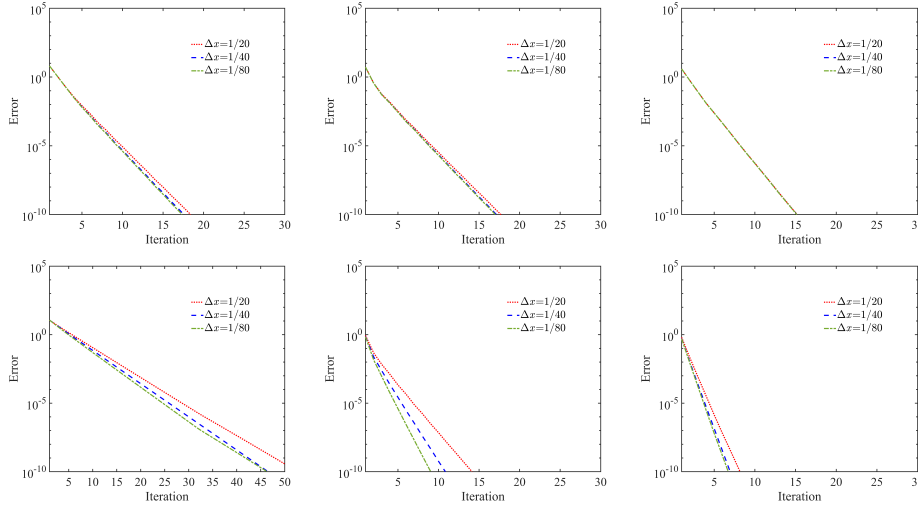


FIG. 9. Convergence behavior of the three local transmission conditions with a given time step $\Delta t = \frac{1}{40}$ and three different mesh size $\Delta x = [\frac{1}{20}, \frac{1}{40}, \frac{1}{80}]$. Top: $\frac{\nu_1}{\nu_2} = 10$. Bottom: $\frac{\nu_1}{\nu_2} = 10^3$. Left: Version I. Middle: Version II. Right: Version III.

652 decomposition with three subdomains,

653
$$\Omega_1 = (0, \frac{1}{5}), \quad \Omega_2 = (\frac{1}{5}, \frac{2}{5}), \quad \Omega_3 = (\frac{2}{5}, 1),$$

654 with Ω_1 the metallic skin, Ω_2 the strain isolation pad, and Ω_3 the thermal insulation
 655 material. In order to imitate differences in the heat diffusion coefficient between
 656 different materials, the heat diffusion coefficients of these three subdomains are set to
 657 1, 10^{-2} , and 10^{-3} , respectively. In practice, the external temperature of the thermal

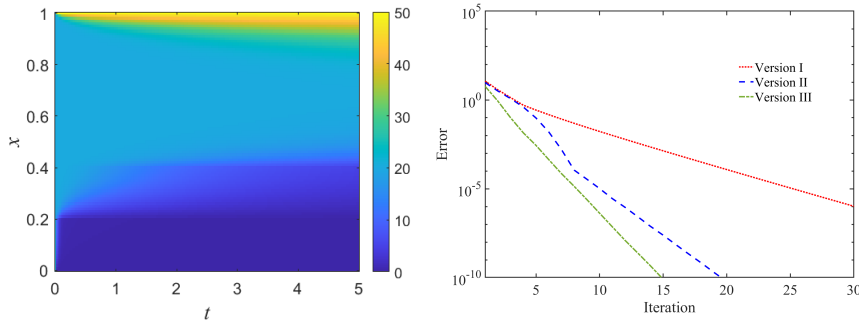


FIG. 10. *Solution of the heat distribution within a thermal protection structure (Left) and convergence behavior of the three local transmission conditions with three asymmetric subdomains (Right).*

658 insulation materials is high. Hence, to account for this, we take the Dirichlet boundary
 659 conditions $g_3 = 50$ at $x = 1$ in Ω_3 and $g_1 = 0$ at $x = 0$ in Ω_1 . We set the mesh size
 660 $\Delta x = 1/100$, the time step $\Delta t = 1/40$ and keep the same initial condition $u_0 = 20$.

661 The solution of the heat distribution is illustrated in Figure 10 on the left. Com-
 662 pared to the behavior in Ω_2 and Ω_3 , we observe that the heat diffuses quite fast in
 663 Ω_1 and goes rapidly to 0. However, since the heat diffusion coefficient is rather small
 664 in Ω_3 , it will prevent the high temperature at $x = 1$ from passing through the ther-
 665 mal insulation material. Furthermore, the convergence behavior of the three local
 666 transmission conditions is also presented in Figure 10 on the right. In this case with
 667 asymmetric subdomains, we observe that the convergence behavior of Versions II and
 668 III is much better than that of Version I, and Version III is the best among them.
 669 This is consistent with our previous numerical experiments, and shows that our ana-
 670 lytical results for the two-subdomain case can provide appropriate local transmission
 671 conditions to accelerate the simulation of more general heat transfer problems within
 672 typical thermal protection structures.

673 **6. Conclusion.** We analyzed at the continuous level the optimized Schwarz
 674 method applied to heat transfer problems with discontinuous diffusion coefficients. We
 675 considered two nonoverlapping subdomains and optimized the transmission conditions
 676 to accelerate the convergence of the iteration. To obtain good local approximations
 677 of the transmission parameters, three local transmission parameters were studied. By
 678 solving the min-max problem associated with each transmission condition, we ob-
 679 tained analytical formulas for the optimized transmission parameters. These analyses
 680 can also be extended to higher dimension by using Fourier techniques, following tech-
 681 niques for the constant coefficient case in [2]. Numerical examples demonstrated that
 682 the optimized transmission conditions with an appropriate scaling are very effective
 683 and stable, and provide better convergence when the diffusion coefficient has a large
 684 discontinuity. However, the performance of all three local transmission conditions
 685 becomes rather similar when the discontinuity becomes small. In addition, we also
 686 observe in our numerical experiments that both the mesh size and the time step can
 687 influence the convergence, especially when the transmission parameters are not well
 688 scaled with respect to the diffusion coefficients. To better understand the dependency
 689 of the convergence on the mesh size and the time step, one needs to analyze the
 690 optimized Schwarz method of the discrete level in the time and space directions for
 691 such heat transfer problems. From a practical viewpoint, we showed that Version

692 III can be used to obtain effective and robust transmission conditions to solve heat
 693 transfer problems with heterogeneous diffusion coefficients. Moreover, the numerical
 694 experiment with asymmetric decomposition and multiple subdomains also reveals the
 695 potential of the present method for realistic thermal protection structures.

696 **Acknowledgments.** We greatly appreciate the anonymous reviewers for their
 697 valuable remarks and comments. It helped a lot to improve the clarity of the paper.

698

REFERENCES

- 699 [1] J. ANDERSON, *Hypersonic and high temperature gas dynamics*, New York, McGraw-Hill, 1989.
 700 [2] D. BENNEQUIN, M. GANDER, L. GOUARIN, AND L. HALPERN, *Optimized Schwarz waveform re-*
 701 *laxation for advection reaction diffusion equations in two dimensions*, *Numerische Math-*
 702 *ematik*, 134 (2016), pp. 513–567.
 703 [3] P. BIRKEN, M. GANDER, AND N. KOTARSKY, *Continuous analysis of waveform relaxation for*
 704 *heterogeneous heat equations*. Submitted, 2024.
 705 [4] E. DIVO, A. KASSAB, AND F. RODRIGUEZ, *Parallel domain decomposition approach for large-*
 706 *scale three-dimensional boundary-element models in linear and nonlinear heat conduction*,
 707 *Numerical Heat Transfer, Part B*, 44 (2003), pp. 417–437.
 708 [5] O. DUBOIS AND M. GANDER, *Optimized Schwarz methods for a diffusion problem with discon-*
 709 *tinuous coefficient*, *Numerical Algorithms*, 69 (2015), pp. 109–144.
 710 [6] W. FENG, K. YANG, M. CUI, AND X. GAO, *Analytically-integrated radial integration bem for*
 711 *solving three-dimensional transient heat conduction problems*, *International Communica-*
 712 *tions in Heat and Mass Transfer*, 79 (2016), pp. 21–30.
 713 [7] M. GANDER, *Schwarz methods over the course of time*, *Electronic Transactions on Numerical*
 714 *Analysis*, 31 (2008), pp. 228–255.
 715 [8] M. GANDER, F. KWOK, AND B. MANDAL, *Dirichlet–Neumann and Neumann–Neumann wave-*
 716 *form relaxation algorithms for parabolic problems*, *Electronic Transactions on Numerical*
 717 *Analysis*, 45 (2016), pp. 424–456.
 718 [9] M. GANDER AND T. LUNET, *Time Parallel Time Integration*, Society for Industrial and Applied
 719 Mathematics, Philadelphia, PA, 2024.
 720 [10] M. GANDER AND T. VANZAN, *Heterogeneous optimized Schwarz methods for second order el-*
 721 *liptic PDEs*, *SIAM Journal on Scientific Computing*, 41 (2019), pp. A2329–A2354.
 722 [11] L. GERARDO-GIORDA AND F. NATAF, *Optimized Schwarz methods for unsymmetric layered*
 723 *problems with strongly discontinuous and anisotropic coefficients*, *Journal of Numerical*
 724 *Mathematics*, 13 (2005), pp. 265–294.
 725 [12] M. GIRAULT AND D. PETIT, *Identification methods in nonlinear heat conduction. part I: model*
 726 *reduction*, *International Journal of Heat and Mass Transfer*, 48 (2005), pp. 105–118.
 727 [13] ———, *Identification methods in nonlinear heat conduction. part II: inverse problem using a*
 728 *reduced model*, *International Journal of Heat and Mass Transfer*, 48 (2005), pp. 119–133.
 729 [14] P. GOLDFELD, L. PAVARINO, AND O. WIDLUND, *Balancing Neumann–Neumann precondition-*
 730 *ers for mixed approximations of heterogeneous problems in linear elasticity*, *Numerische*
 731 *Mathematik*, 95 (2003), pp. 283–324.
 732 [15] S. KUMAR AND S. MAHULIKAR, *Selection of materials and design of multilayer lightweight pas-*
 733 *sive thermal protection system*, *Journal of Thermal Science and Engineering Applications*,
 734 8 (2016), p. 021003.
 735 [16] ———, *Design of thermal protection system for reusable hypersonic vehicle using inverse ap-*
 736 *proach*, *Journal of Spacecraft and Rockets*, 54 (2017), pp. 436–446.
 737 [17] F. LEMARIÉ, L. DEBREU, AND E. BLAYO, *Toward an optimized global-in-time Schwarz algo-*
 738 *rithm for diffusion equations with discontinuous and spatially variable coefficients. Part 1:*
 739 *the constant coefficients case*, *Electronic Transactions on Numerical Analysis*, 40 (2013),
 740 pp. 148–169.
 741 [18] ———, *Toward an optimized global-in-time Schwarz algorithm for diffusion equations with*
 742 *discontinuous and spatially variable coefficients. Part 2: the variable coefficients case*,
 743 *Electronic Transactions on Numerical Analysis*, 40 (2013), pp. 170–186.
 744 [19] Y. MADAY AND F. MAGOULÈS, *Optimized Schwarz methods without overlap for highly hetero-*
 745 *geneous media*, *Computer Methods in Applied Mechanics and Engineering*, 196 (2007),
 746 pp. 1541–1553. *Domain Decomposition Methods: recent advances and new challenges in*
 747 *engineering*.
 748 [20] H. SCHWARZ, *Über einen Grenzübergang durch alternierendes Verfahren*, *Vierteljahrsschrift der*
 749 *Naturforschenden Gesellschaft in Zürich*, 15 (1870), pp. 272–286.

- 750 [21] O. UYANNA AND H. NAJAFI, *Thermal protection systems for space vehicles: A review on*
751 *technology development, current challenges and future prospects*, Acta Astronautica, 176
752 (2020), pp. 341–356.
- 753 [22] B. ZHANG, J. MEI, M. CUI, X.-W. GAO, AND Y. ZHANG, *A general approach for solving three-*
754 *dimensional transient nonlinear inverse heat conduction problems in irregular complex*
755 *structures*, International Journal of Heat and Mass Transfer, 140 (2019), pp. 909–917.